



HAL
open science

The Fission Yeast Mating-Type Switching Motto: “One-for-Two” and “Two-for-One”

Benoît Arcangioli, Serge Gangloff

► To cite this version:

Benoît Arcangioli, Serge Gangloff. The Fission Yeast Mating-Type Switching Motto: “One-for-Two” and “Two-for-One”. *Microbiology and Molecular Biology Reviews*, 2023, Sex in Fungi, 10.1128/membr.00008-21 . hal-04010024

HAL Id: hal-04010024

<https://hal.science/hal-04010024v1>

Submitted on 2 Mar 2023

HAL is a multi-disciplinary open access archive for the deposit and dissemination of scientific research documents, whether they are published or not. The documents may come from teaching and research institutions in France or abroad, or from public or private research centers.

L'archive ouverte pluridisciplinaire **HAL**, est destinée au dépôt et à la diffusion de documents scientifiques de niveau recherche, publiés ou non, émanant des établissements d'enseignement et de recherche français ou étrangers, des laboratoires publics ou privés.



Distributed under a Creative Commons Attribution 4.0 International License



The Fission Yeast Mating-Type Switching Motto: “One-for-Two” and “Two-for-One”

 Benoit Arcangioli,^a  Serge Gangloff^{a,b}

^aGenome Dynamics Unit, Genomes and Genetics Department, Pasteur Institute, Paris, France

^bUMR3525, Genetics of Genomes, CNRS-Pasteur Institute, Paris, France

SUMMARY	1
INTRODUCTION	1
TWO MATING STRATEGIES	2
TWO LIFE CYCLES: MATING VERSUS QUIESCENCE	4
TWO CONSECUTIVE ASYMMETRIC CELL DIVISIONS	5
TWO SILENT DONORS AND ONE EXPRESSED ACCEPTOR	7
THE SITE- AND STRAND-SPECIFIC <i>MAT1</i> IMPRINT	7
THE IMPRINT IS MADE DURING <i>MAT1</i> DNA REPLICATION	10
<i>CIS</i> - AND <i>TRANS</i> -ACTING ELEMENTS REQUIRED FOR PAUSING AND IMPRINTING	12
OTHER REPLICATION FORK BARRIERS	14
MATING-TYPE SWITCHING PROCESS	15
ESTABLISHMENT AND MAINTENANCE OF HETEROCHROMATIN AT THE <i>MAT2/MAT3</i> REGIONS	18
TWO DONORS' CHOICE: DIRECTIONALITY OF SWITCHING	20
CONCLUDING REMARKS	21
ACKNOWLEDGMENTS	22
REFERENCES	22

SUMMARY *Schizosaccharomyces pombe* is an ascomycete fungus that divides by medial fission; it is thus commonly referred to as fission yeast, as opposed to the distantly related budding yeast *Saccharomyces cerevisiae*. The reproductive lifestyle of *S. pombe* relies on an efficient genetic sex determination system generating a 1:1 sex ratio and using alternating haploid/diploid phases in response to environmental conditions. In this review, we address how one haploid cell manages to generate two sister cells with opposite mating types, a prerequisite to conjugation and meiosis. This mating-type switching process depends on two highly efficient consecutive asymmetric cell divisions that rely on DNA replication, repair, and recombination as well as the structure and components of heterochromatin. We pay special attention to the intimate interplay between the genetic and epigenetic partners involved in this process to underscore the importance of basic research and its profound implication for a better understanding of chromatin biology.

KEYWORDS DNA recombination, DNA replication, fission yeast, heterochromatin

INTRODUCTION

The fission yeast *Schizosaccharomyces pombe* was isolated over 100 years ago from African millet beer by the German chemist and microbiologist Paul Lindner (1893) (1) and was later used as a model organism by Leupold, Mitchison, and Robinow in the 1950s to describe the initial steps of mitotic and meiotic divisions. Indeed, early microscopic observation had indicated that the fusion of two sister cells is rapidly followed by meiosis and sporulation (2–4). This simple inspection encouraged many subsequent studies that have led to the notion of mating-type switching (MTS) in *S. pombe*.

Vegetatively growing *S. pombe* cells exhibit a cylindrical rod shape of 4 μm in diameter with a length ranging between 7 and 14 μm . The cells grow by elongation, and

Copyright © 2023 American Society for Microbiology. All Rights Reserved.

Address correspondence to Benoit Arcangioli, benoit.arcangioli@pasteur.fr.

The authors declare no conflict of interest.

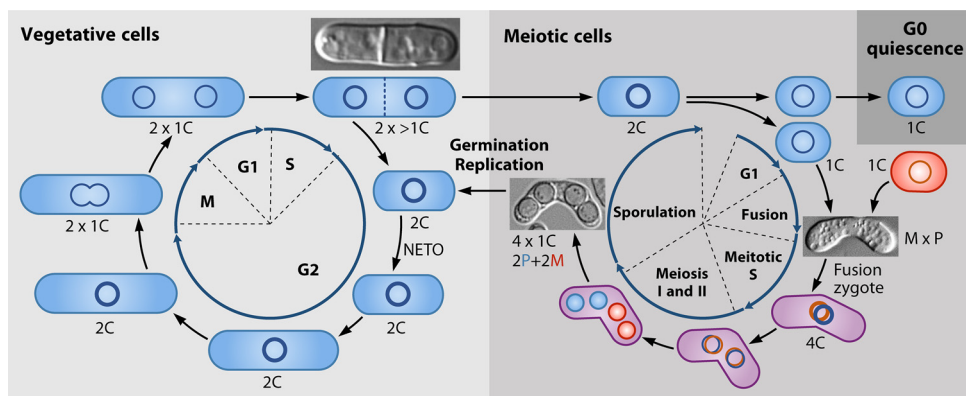


FIG 1 *S. pombe* cell cycle. (Left) Vegetative cycle (light gray area). Septation is concomitant with S phase, and thus most of the cells in a growing population contain a nucleus with a 2C DNA content. The sister cells resume growth only by the old ends located at the opposite side of the cytokinesis site. The transition from monopolar to bipolar growth is called NETO (new-end takeoff). G₂ is the longest phase of the cell cycle during vegetative growth, and the lengths of M, G₁, and S are roughly the same. The thicknesses of the lines of the nuclei reflect the amounts of DNA present. (Right) When cells experience starvation, the meiotic cycle is triggered (darker gray area) and cells engage a single DNA replication and two rapid cell divisions and arrest in G₁. Note that only one daughter cell is depicted following the S phase in both the vegetative and meiotic cycles. After G₁ arrest, cells enter the G₀/quiescent state. Two G₁ cells with complementary MTs conjugate (blue and other) and form a diploid and a zygote that undergoes meiosis, followed by sporulation that gives rise to four ascospores (2P and 2M), which upon germination and DNA replication can enter the vegetative cycle. The nuclear DNA content of different cell types and the phases of vegetative and meiotic cycles are indicated.

the medial position of the septum generates two sister cells of comparable length, a feature that led to the common name of “fission yeast.” Currently, many researchers are working on numerous molecular and cellular aspects of *S. pombe* and its closest relatives, including *Schizosaccharomyces octosporus*, *S. cryophilus*, *S. osmophilus*, and the more distant dimorphic *S. japonicus* (5). All *S. pombe* or fission yeast strains referred to in this review are derived from the haploid wild-type strain 972h– (6, 7).

Fission yeast spends most of its time as a unicellular haploid cell that exists under two exclusive mating types (MTs), minus (M) and plus (P), and mating is only possible between strains of different types. When both MT partners (M and P cells) are in close proximity, they conjugate and generate a zygote. The diploid state is only a transient step to meiosis that generates four haploid spores in an ascus. Cell growth and cell division are intimately coordinated by the conserved cyclin-dependent kinase Cdc2 to maintain size and ploidy, which delineate the phases of the cell cycle (8). In a cycling population, 70% of the cells are in G₂, while cells in G₁, S, and M phases account for 10 to 15% each (Fig. 1). Importantly, mitosis separates the nuclei that reside in the same cell body. DNA replication is concomitant with the formation of the septum and separates the sister cells to produce two cells in G₂ (2C DNA content). As a consequence, examination of the DNA content by flow cytometry of an exponential phase growing culture appears homogenous with a 2C DNA content. When cells reach a critical size (14 μm) at the late G₂ phase, they stop elongating and enter mitosis, which is rapidly followed by a short G₁ phase and the onset of DNA replication coupled with both the assembly of a new membrane and the formation of a septum in the middle of the cell to physically separate two sister cells of the identical size. Cytokinesis concludes with the cleavage of the primary septum liberating two new ends facing one another. After cell division, the cells are at the end of S phase or in G₂ and the sister cells resume growth only by the old ends located at the opposite side of the cytokinesis site. The transition from monopolar to bipolar growth is called NETO (new-end takeoff) (9, 10) and requires DNA replication completion (11).

TWO MATING STRATEGIES

S. pombe exists as heterothallic or homothallic strains, concepts derived from filamentous fungi (thallus). Each form has its own mating strategy. From a single spore (or cell),

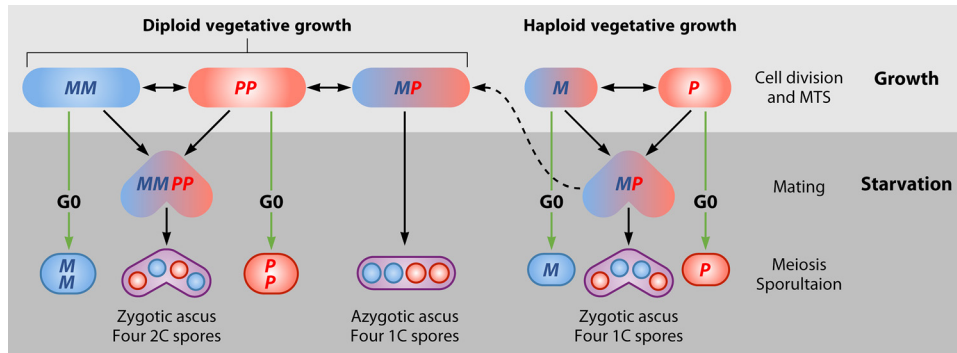


FIG 2 *S. pombe* life cycle. Under growth conditions (light gray area), haploid and transient diploid homothallic strains switch their mating type, as indicated by double arrows. When cells experience starvation (dark gray area), mating activities are induced and, in the absence of partners, cells enter G₀ (green arrows), whereas in the presence of alternative mating-type partners, they undergo mating, meiosis, and sporulation. When the diploid zygotes encounter favorable growth conditions, they can resume cell division, as shown by a curly dashed line. Under growth conditions, the ascospores germinate to resume the asexual vegetative life cycle. Note that two different shapes correspond to zygotic and azygotic asci.

heterothallic strains produce a clonal population of cells with a unique MT, whereas homothallic strains produce a population containing a mixture of P and M cells in similar proportions produced by MTS. The mating phenotype of the cells is revealed by environmental cues, in particular nitrogen availability, which triggers the major developmental decision that brings about a transition from mitotic cell division to two reversible resting states. When only one MT is present, sexual activity is impossible and cells arrest in quiescence (Fig. 1 and 2), readjusting numerous important genetic and metabolic regulations (12–14). When the alternative MT cells are present, they mate and form a diploid cell that undergoes meiosis and sporulation, thus generating four dormant haploid spores. While quiescent cells are more resistant to stress than growing cells, spores exhibit the best resistance to extreme conditions (15). The mitotically dividing haploid heterothallic and homothallic cells are indistinguishable, and the M-P cell types or gametes are also morphologically identical (isogamy). They reveal their gametic potential only under starving or stressful conditions (Fig. 2). In contrast, gametes produced by multicellular organisms are called male and female and they can be distinguished by their size or form (anisogamy) (16). Because a clonal population of a heterothallic subtype is made of cells with a single MT, they are also called cross-fertile (or self-sterile). In the absence of motility, their sexual reproduction requires the “search” of cells with the opposite MT using a third party. However, when the homothallic strain experiences starvation, it mates and produces roughly 90% of spores, a proportion at the origin of the name h^{90} of this self-crossing subtype. The h^{90} strain can spontaneously generate both types of heterothallic strains at a low frequency (10^{-3} to 10^{-4}) corresponding to genetic accidents/errors during the process of MTS. Their molecular nature has been described previously (17). The homothallic strain is slightly more abundant in nature and is commonly proposed as the wild-type strain (18). The *S. pombe* ascospores contain starch that stains darkly when exposed to iodine vapors (see below in Fig. 4B). This iodine staining is a simple and convenient procedure to distinguish spores in individual colonies and to identify homothallic from heterothallic strains directly on a petri dish.

The genetic advantage of one strategy over the other one in surviving adverse conditions is not obvious. Upon starvation, homothallic strains can readily generate long-lived spores upon mating between sister or cousin cells (inbreeding), thereby producing no or low genetic variability. Under similar starvation conditions, a clonal heterothallic cell population cannot mate to produce spores and will arrest in the quiescent state. When the conditions become suitable again, the quiescent cells reenter the vegetative cycle faster than spores (no germination) and will therefore benefit from the available nutrients to expand their colony size. This situation frequently occurs in the laboratory, where aging colonies emanating from a homothallic cell will tend to accumulate heterothallic variants that will gradually dominate the parental homothallic cell population after reseeded. On the other

hand, if the period of starvation persists, the dormant spores with a high survival rate provide an advantage to the homothallic strain. However, heterothallic or homothallic strains can interbreed and form spores if they express complementary MTs. Mendelian distorting elements, such as the *wtf* gene family, increase their transmission to progeny between nonclonal populations. Their meiotic drive features have been used to support inbreeding over outcrossing. However, both population evolution and experimental studies have indicated frequent outcrossing in natural isolates and an active role of heterothallic strains in fission yeast evolution (19–22). For both subtypes, the “search” for partners from a different lineage remains the only solution to produce genetic variability for a better-adapted offspring. We still know very little about the *S. pombe* ecology (5, 18, 23), but in the absence of motility, it is conceivable that the mating partner can be found in the gut of fruit-fed animals, honey, or fermented products (24, 25). Thus, it appears that the production of homothallic and heterothallic yeast subtypes offers alternative and complementary advantages in a rapidly changing environment and provides an optimized solution over time.

TWO LIFE CYCLES: MATING VERSUS QUIESCENCE

Nitrogen starvation has been extensively used to study cell cycle arrest, mating, meiosis, and quiescence in fission yeast (26, 27). The absence of nitrogen is rapidly sensed by TOR (target of rapamycin) signaling and the stress/mitogen-activated protein kinases (S/MAPK). This triggers two rapid cell divisions with one round of DNA replication that allows the cells to arrest safely in pre-Start G₁ with a one-cell (1C) content by engaging Polo kinase and the cyclin-dependent protein kinase (CDK). The main actors of this arrest are the cyclin kinase inhibitor Rum1 and the anaphase-promoting complex/cyclosome (APC/C) activator Ste9 (28). The sequence of events leading to G₀ entry is well conserved in eukaryotes. In fission yeast, haploid cells arrest with a 1C DNA content before engaging in quiescence or sexual differentiation (Fig. 1). During this process, the Styl S/MAP kinase phosphorylates transcription factor Atf1, which triggers massive changes in gene expression, including the transcriptional activation of the master transcription factor Ste11 required to reveal the cell-type identity and to commit to the gametogenesis program (29, 30). The Ste11 protein is a sequence-specific DNA-binding high mobility group (HMG) box protein that binds to more than 80 promoters. Some targets are different in M and P cells, reflecting the differential association of Ste11 with the M- and P-specific transcription factors triggering the expression of the P and M pheromones and their respective receptors (30, 31). While transcriptional controls ensure that Ste11 is transcribed at a high level only when nutrients are scarce, posttranscriptional controls limit its function to the G₁ phase of the cell cycle, where the differentiation program is initiated. Expression of Ste11 targets establishes pheromone signaling between cells of different MTs, and several transcriptional feedback loops ensure that the cell fate decision is irreversible (32).

The *mat1-P* cassette contains two diverging *Pc* and *Pi* genes, while the *mat1-M* cassette contains the *Mc* and *Mi* genes, with *c* and *i* standing for constitutive and inducible, respectively (33) (see below in Fig. 4A). They encode transcription factors. *Mc* codes for a single HMG box protein highly similar to the SRY protein that transcriptionally controls male development in mammals (34). In M cells, the *Mc* and Ste11 HMG proteins associate to activate M-specific genes. In P cells, *Pi* contains a homeobox with a Three Amino acid Loop Extension between helix 1 and helix 2 called TALE that is well conserved in fungi and beyond (35). *mat1-Pc* and *mat1-Mc* are weakly and constitutively transcribed during growth, while *mat1-Pi* and *mat1-Mi* are not detected. The four genes are induced via Ste11 during starvation. *Mat1-Mc* interacts with Ste11 while *Mat1-Pc* interacts with Map1, a MAD box transcription factor, and both complexes activate the expression of their respective pheromone and pheromone receptor genes (36, 37).

Cell agglutination is an early response to stress that brings the cells close to each other, enhancing the action of the pheromones/receptors that guide cellular mating, and leads to the successful fusion between mating partners (38). Numerous studies

have reported how complementarities and asymmetries between M and P cell types have evolved to optimize mating specificity and efficiency (39). Next, the pheromone cascade activates *mat1-Pi* and *mat1-Mi* factors. To improve monogamous mating in a crowded cellular environment, a cell with multiple partners can orient stably only toward a single one, and a single merge is favored by an asymmetry in turgor pressure ($M > P$) in the two partners. Immediately after the fusion of the cytoplasm, but still with two distinct nuclei, the small Mi protein rapidly diffuses into the cytoplasm of the P cell and is captured by the nuclear P cell-specific homeobox protein Pi to trigger zygotic transcription from the P genome. As a consequence, the meiotic master gene *mei3* is first transcribed from the P genome and next from the M genome (40), followed by the activation of *mei2* that blocks refertilization to restrict meiosis to two partners (41, 42). Thus, the two fission yeast gametes, although appearing isogamous at the cellular level, have already evolved subtle asymmetric strategies that may foreshadow the beginning of a commitment to sexual dimorphism.

Since the diploid phase is only transient, *S. pombe* spends most of its time as a haploid and exhibits a haplophasic or haplontic life cycle. However, under laboratory conditions, the diploid state can be artificially extended by adding nitrogen sources between mating and the onset of meiosis prior to the Ste11 commitment to trigger the reentry into the vegetative cycle (Fig. 2). The diploid cell population can be selected and maintained using complementary intragenic markers. However, even under these conditions, the diploid cells are fragile, with limited viability. This fragility can be revealed at the colony level on a petri dish containing the red dye phloxine B. The high proportion of dead cells in a diploid colony is used to distinguish haploid strains that appear white/pink and diploids strains that stain red (43).

The sexual cycle is not the only solution when cells experience starvation. When a population is made of a single MT (heterothallic) or when cells are rapidly diluted, mating is not an option anymore. In the absence of nitrogen, fission yeast has developed a genetic program to safely enter into a quiescent state (13, 44, 45) whereby two rapid cell divisions with no elongation of the cells convey it to G₁, then to G₀/quiescence (Fig. 2). In this state, the cells are more resistant to stress, are metabolically active, and ensure the homeostasis of the genetic material (46, 47). The knowledge of the genetics of quiescence is progressing rapidly and has revealed that time is as strong a vector as DNA replication to generate mutations and to fuel evolution (48).

TWO CONSECUTIVE ASYMMETRIC CELL DIVISIONS

Conjugation between homothallic sister cells indicating a rapid and efficient MTS process, at least when cells are approaching nutritional starvation, was reported over a century ago (2). A series of cell pedigrees (4, 49, 50) established to monitor the mating process under conditions close to starvation using haploid cells has revealed that MTS is not random but follows specific rules. MTS requires two consecutive asymmetric cell divisions. The first division leads to switchable (s) and unswitchable (u) daughter cells; here, the asymmetry is inferred and resides in the potential of switching that is revealed only during the following cell division. The second division leads to MTS in the switchable daughter cell, which can be monitored through the mating and formation of zygotic asci by microscopy.

This cell lineage generates one switched cell out of 4 cousin cells and was called the “one-in-four” or Miyata rule (4) (Fig. 3A). This simple result raised two basic questions. How can only one sister inherit the potential for switching at the next cell division and how can only one sister cell switch its MT? The switching pedigree using haploid cells makes it impossible to track the fate of the sister of the switched cell because it is involved in mating with it, but the diploid cells make it possible to overcome this problem.

A freshly made diploid cell heterozygous at *mat1* (*M/P*) can be maintained in growing conditions and the switching efficiency can be studied during starvation by monitoring azygotic asci formation in a lineage. The frequent occurrence of *MM* or *PP* diploid cells unable to sporulate but able to divide (Fig. 2) suggests that the competence for

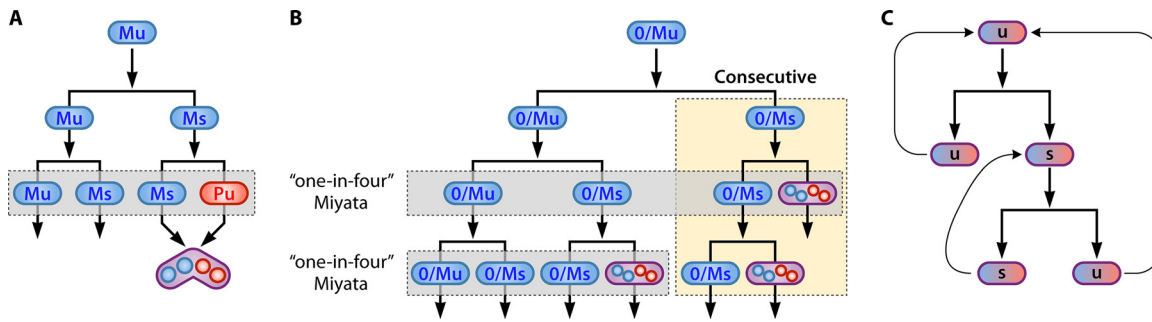


FIG 3 Mating-type switching patterns in haploids and diploids. (A) Haploid cell lineage monitoring the mating between two sister cells and ascus formation. The unswitchable Mu cells produce two M cells, while the switchable Ms cells produce a switched P cell identified by the formation of a zygotic ascus. The suffix “s” can be inferred only after the production of an ascus. Otherwise, it is labeled “u.” The Mu cells produce four cousins containing a single switched progeny according to the Miyata rule or the “one-in-four” switching rule. (B) Diploid cell lineage of the *mat1-Msmt0/mat1-M* strain (O/M). The stable *mat1-Msmt-0* allele (not indicated) allows the monitoring of the switching of the *mat1-M* allele (indicated). In the diploid configuration, the switching is monitored by the formation of an azygotic ascus. The lineage of the Ms cells generates a chain of recurrent switching called the “consecutive” switching rule. (C) The switching pattern is characteristic of stem cell division, producing two different daughter cells: one identical to the parent and one with a new fate. The first asymmetry relies on the process of imprinting/licensing one DNA strand at *mat1*, and the second relies on the process of recombination/repair of the imprint generating MTS. A similar pedigree was observed in M or P cells, indicating that both *mat1-M* and *mat1-P* follow the same process. The back arrows indicate the fate of the upcoming progeny.

switching operates at the level of individual chromosomes, ruling out a cytoplasmic determinant for this asymmetry (49–51). Unfortunately, the frequency of switching and the inability to distinguish the chromatids make it difficult to establish the MT switching pedigree. However, this impediment was overcome by using diploid strains in which one of the *mat1* alleles never switches because it contains a small cis-acting deletion that blocks switching (called *mat1-Msmt-0* or *mat1-P Δ 17*, and further described below), while the other *mat1* allele is free to switch. The diploid *mat1-Msmt-0/mat1-M* grows slowly on plates containing a low concentration of nitrogen, whereas the diploid *mat1-Msmt-0/mat1-P* forms an ascus that is easily distinguishable under microscopic scrutiny (Fig. 3B).

By following the formation of asci in a pedigree, the “one-in-four” switching rule was confirmed. In addition, it was observed that the sister of the switched cell is switchable again during the following cell division, thus generating a chain of consecutive switching. The efficiencies of the “one-in-four” and “consecutive” rules (Fig. 3B) are similar and close to 90%, indicating that the switching uses primarily the opposite MT. Thus, this activity rapidly generates a 1:1 sex ratio in emerging colonies and brought about the idea of a process designated “directionality of switching” (52). Furthermore, several *cis*- and *trans*-acting switching mutants that are described below reduce both switching rules to the same extent, suggesting that the two asymmetric divisions use the same process (53, 54). An exception to the “one-in-four” MTS patterns was provided by the haploid strain containing an inverted tandem duplication of *mat1* (see below). In this strain, the two *mat1* cassettes switch separately and generate two switchable cells in a lineage. While most investigators have assumed that the replication of the “Watson and Crick” cDNA strands pass the same information to the daughter cells, Klar’s model proposes that they can be differentially imprinted so that daughter cells inherit different developmental fates (50; reviewed in reference 55). In 1987, several molecular models targeting one of the DNA strands were proposed: a protein complex segregating with a specific DNA strand, a site- and strand-specific nick, and an unrepaired RNA primer of an Okazaki fragment. More recently, fluorescent markers specific to P or M cell types have confirmed the pattern of switching when cells approach starvation but still require further improvement to monitor MTS by fluorescence microscopy during vegetative growth (22, 56, 57).

Taken together, the asymmetric cell division in fission yeast is analogous to the stem cell division described for multicellular organisms. Stem cells are unique in their ability to make intrinsic asymmetric divisions generating sister cells with different fates, one retaining its stem cell potential and the other, which is more advanced in the

differentiation program, generating cellular diversity (Fig. 3C). DNA, RNA, proteins, or organelles have been described as major determinants of asymmetry in eukaryotes. Due to their molecular differences, numerous segregation mechanisms are anticipated (58), including asymmetric epigenetic inheritance (59). In *S. pombe*, the asymmetry is carried by haploid cells that produce the two complementary gametes. The different fate of the sister cells is intrinsic and is thought to be induced by the unequal segregation of master determinants. It is important to note, however, that extrinsic cues acting mainly on the cell cycle or growth machinery are central to reveal but not to generate the potential of the sister cells following asymmetric cell division. This is the case for nitrogen starvation, which triggers the expression of the allele present at *mat1*. The initial observation of the mating of sister cells implicitly proposes a precise timing between DNA replication and recombination leading to MTS. We discuss below the active role of DNA replication/repair/recombination in two epigenetic processes that helped our understanding of this well-studied and original asymmetric cell division mode (for a review, see reference 60).

TWO SILENT DONORS AND ONE EXPRESSED ACCEPTOR

The *S. pombe* genome resides on three chromosomes for a total of 14 million base pairs, which were sequenced in 2002 (23). The sequence organization of the MT region has provided important information on the molecular strategy used for MTS. The MT region is located on the right arm of chromosome 2 and spans 30 kb (61, 62) (Fig. 4A). The names and locations of the components are indicated below, and their functions in MTS are described further in the following sections.

In the homothallic strain, the MT region contains three related cassettes of about 1 kb in length: *mat1* harboring either the M or the P allele, *mat2-P*, and *mat3-M*. The three cassettes are each flanked by two short homology boxes, one of 59 bp to the right (H1) and one of 135 bp to the left (H2). A third box of 57 bp (H3) is present only at the two silent loci, to the left of H2 (Fig. 4A). These short boxes of homology are used for base pairing during the initiation and resolution steps of the gene conversion process leading to MTS and are discussed below. In vegetative growth, the MT of the cell is phenotypically invisible and can be revealed only molecularly. The *mat1* locus contains an efficient origin of replication on its centromere distal side and is flanked by two strong replication fork pause sites, which are described below (17). The *mat2-P* and *mat3-M* cassettes are embedded in a heterochromatin domain of 20 kb that is silent for transcription and mitotic/meiotic recombination (63–65). Genetically, the *mat2-P* and *mat3-M* cassettes segregate as a single locus (51). Numerous studies have identified functional elements that are instrumental in the choice of donors in the process of MTS. Since they are used as a DNA template during the MTS process, the two silent cassettes are the donors of genetic information, while the *mat1* cassette is the acceptor. Two Swi2-dependent recombination enhancers named SRE2 and SRE3 have been found near *mat2* and *mat3* and are involved in the choice of the donors. The *mat1* and *mat2-P* cassettes are separated by the 15-kb-long L region, and *mat2-P* and *mat3-M* cassettes are separated by the 11-kb-long K region. The middle of the *mat2-P* and *mat3-M* interval contains the 4.3-kb *cenH* array made of the *dg* and *dh* repeats, which are also present at centromeres and responsible for heterochromatin nucleation (66). Two additional repressor elements, named REII and REIII, next to *mat2-P* and *mat3-M*, respectively, induce a weaker nucleation effect and serve as a relay to reinforce the silencing power of the constitutive heterochromatin provided by *cenH* (67–70). Finally, the silent region is flanked by two boundary elements made of 2-kb inverted repeats, IR-L and IR-R (71–73). The synergistic action between the repetitions suggests the formation of a chromatin loop anchored at the base by the inverted repeats and exposing the *cenH* nucleation center (72).

THE SITE- AND STRAND-SPECIFIC MAT1 IMPRINT

Southern blot hybridization of genomic DNA from homothallic strains showed that

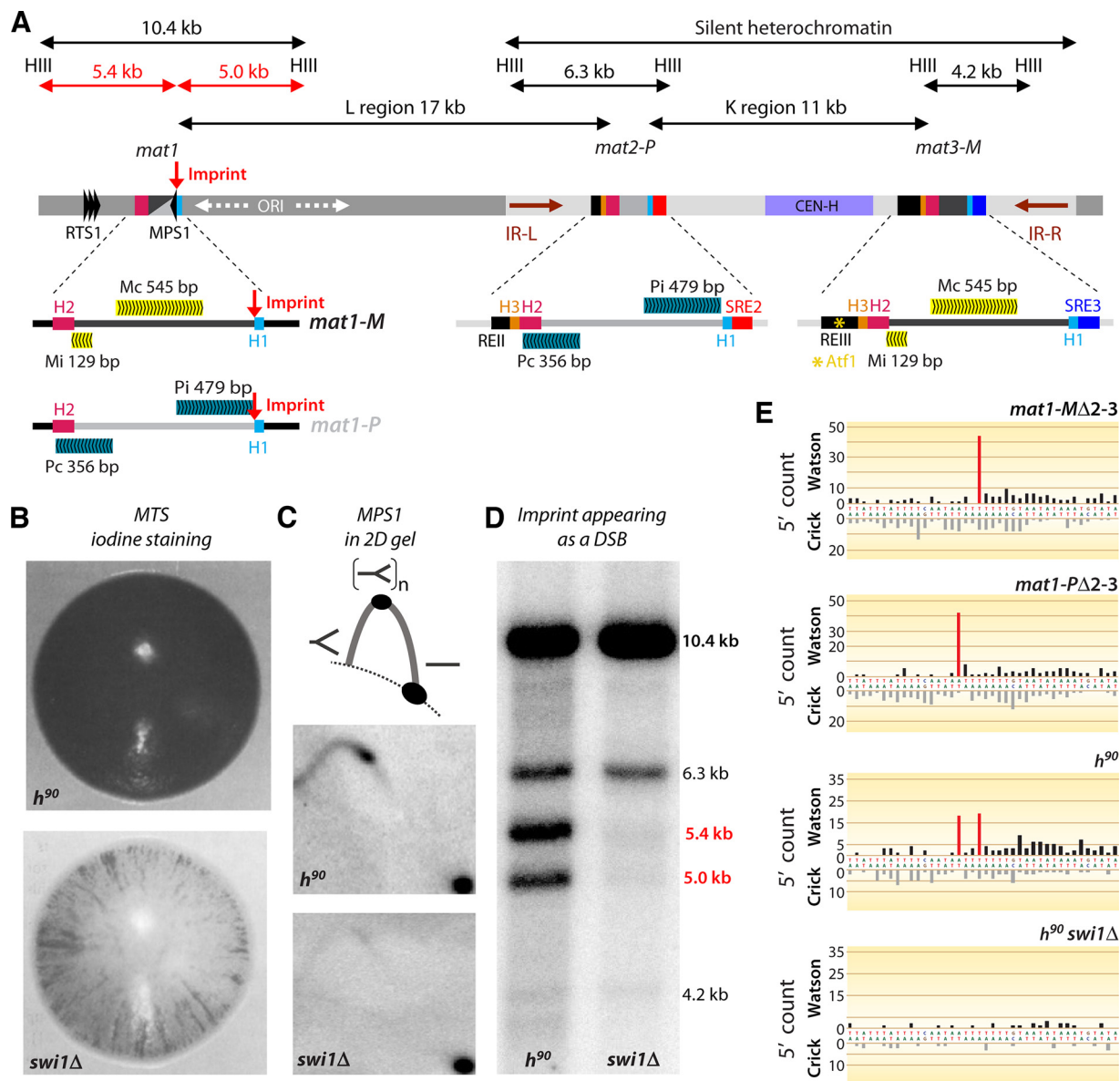


FIG 4 Organization of the *mat* region and detection of mating-type switching. (A) Schematic of the *mat* region on chromosome 2 highlighting the major functional components. *HindIII* refers to a restriction site digested by *HindIII*. The centromere is located to the left. The known functions of the various elements are indicated in the main text. (B) Iodine staining of colonies capable of switching, mating, and sporulating (h^{90}) or severely impaired in the process ($swi1\Delta$). (C) Fork pausing at *MPS1* determined by 2D gel electrophoresis. Digestion of the *mat1* locus on both sides of *MPS1* was probed with the M allele. (D) Quantification of nicked molecules by Southern blotting of total DNA vortexed and digested with *HindIII* before electrophoresis. The percentage of broken molecules is calculated by adding the intensity of the 5.0-kb and 5.4-kb signals and by dividing it by the total signal (10.4 kb + 5.4 kb + 5.0 kb). The 6.3-kb and 4.2-kb bands are cross-reacting signals from the *mat2* and *mat3* regions, respectively, overlapped by the *HindIII*-*HindIII* probe containing *mat1-P* information. (E) Selective focus on the *mat1* imprinted site. Red bars represent the number of genomic next-generation sequencing (NGS) reads whose 5' end starts at the indicated nucleotide in, from top to bottom, the *mat1-MΔ2-3* strain (no *mat2* or *mat3* information), the *mat1-PΔ2-3* strain (no *mat2* or *mat3* information), the h^{90} strain, and the $h^{90} swi1\Delta$ strain.

a 10.4-kb *HindIII* DNA fragment encompassing *mat1* also includes two subfragments of 5.0 kb and 5.4 kb, regardless of the phase of the cell cycle (62) (Fig. 4D). The broken DNA fragments account for 20 to 40% of the full *HindIII* fragment, and the ends of the broken molecules have been mapped at the nucleotide level in M and P alleles (74). This elevated level of broken molecules has indicated that *mat1* is fragmented in a large proportion of the cells and that the level of breakage is quite stable during the progression of the cell cycle. Pioneering genetic work has identified switching factors (*Swi*) as important for double-strand-break (DSB) formation and involved in the

sequential initiation and resolution steps for MTS (51, 75). Concomitantly, it was shown that the heterothallic strains contain lower levels of breaks at *mat1*, along with specific and stable rearrangements of the donor cassettes (17), supporting the notion that a DSB is the initiating event controlling MTS. At first glance, this situation is similar to that proposed for budding yeast (76, 77), with a DSB initiating MTS. However, later work has shown that the process is very different in every detail. In *Saccharomyces cerevisiae*, the determinant of sexual type asymmetry is cytoplasmic (78) and dictated by the exclusive expression of the HO endonuclease in the mother cell, thus generating a transient DSB at *MAT1* during G_1 . The cleaved *MAT* locus is repaired by using the opposite silent MT before genome duplication and thus generates two sister cells with a switched MT. In the haploid fission yeast, only one of the two daughter cells changes its MT, leading to the proposal that DSB formation and MTS take place during the G_2 phase on only one of the two sister chromatids. Furthermore, the strain deleted for the two donors, *mat2-P* and *mat3-M*, exhibits wild-type levels of DSB at *mat1* and is viable (79, 80), unlike what is observed in *S. cerevisiae*, where the DSB also forms in the absence of donors but results in cell death (81). This result is consistent with a recombinational repair event restricted to the G_2 phase healing the broken chromatid with the intact sister. From this reasoning came the idea of an epigenetic mark restricting the DSB and subsequent MTS to one of the sister chromatids, followed by chromosome segregation and cell division generating a single switched cell.

Soon after, using a tandem duplication of the *mat1* region in an inverted or direct orientation that allows determination of whether sisters differ because of unequal distribution of cytoplasmic and/or nuclear components or because of inheritance of a specific parental DNA chain at the MT locus, Amar Klar proposed the DNA strand-specific imprinting model of which several genetic and molecular aspects are still under study (50). In the inverted and direct orientations, both *mat1* loci are broken. DNA breaks on the same molecule generate a fragment between *mat1* duplications, whereas the absence of fragments indicates breaks on separate molecules. The DNA fragment between the breaks is detected on a Southern blot only in the direct orientation of the duplications, indicating that the breaks arise on the same molecule. Klar concluded that the break determinant is carried by a specific DNA strand at *mat1* (50). In accordance, duplication in the direct orientation is unstable, as both *mat1* loci are simultaneously cleaved on the same chromosome (53). Pedigree studies revealed that both *mat1* cassettes are independently functional in the inverted duplication and exhibit an elevated proportion of "two-in-four" switching patterns. These results imply that a strand-specific imprint at the *mat1* locus leads to a DSB triggering the precise replacement of the *mat1* allele by the opposite allele present in one of the two silent cassettes. Chromosomal imprinting does not alter the DNA sequence and is not mutagenic. It implicates either a covalent modification of one DNA strand or the establishment of a stable complex between a DNA strand and proteins.

At the molecular level, the DSB observed at *mat1* results from the artificial tear of a fragile site during DNA extraction. When *S. pombe* chromosomes are analyzed by pulse-field gel electrophoresis, a broken chromosome II is not observed. In this preparation method, the cells are lysed and maintained in low-melting-point agarose plugs during the entire DNA purification process to preserve the integrity of long DNA molecules. The subsequent HindIII digestion of the locus is also carried out in the plug and generates a 10.4-kb fragment in the absence of the two subfragments of 5.4 and 5.0 kb (Fig. 4D). Finally, the gentle melting of the plugs followed by a vortexing step leads to breakage of a subset of the molecules at a fragile site, yielding two fragments of 5.4 and 5.0 kb. The intensity of the broken fragments relative to the total intensity indicates that 50% of *mat1* is imprinted and behaves as a mechanical fragile site (Fig. 4D). Further analysis using denaturing polyacrylamide gel electrophoresis showed that only one DNA strand is broken at a specific sequence located at the junction between the H1 homology box and the *mat1-M* and *mat1-P* alleles (Fig. 4E) (82). The break is present on 50% of *mat1* molecules and behaves like a fragile site during classical DNA

extraction, thus generating the artifactual DSB through mechanical stress. The position of the single-stranded DNA breaks has been localized to the second T in a run of 7 T's in *mat1-M* or in a run of 10 T's in *mat1-P* alleles (74, 82) (Fig. 4E). In parallel to this work, it was proposed that the nick is an alkali-labile modification of the *mat1* upper strand, leaving the DNA lower strand intact (83). It was anticipated that the imprint is a DNA-RNA-DNA that can be cleaved by a residual RNase during DNA purification. Two populations of imprints with one or two ribonucleotides have been proposed (84, 85).

To explore further the remarkable specificity of the imprint, regardless of it being a "nick" or a ribonucleotide, six PstI restriction sites (CTGCAG) have been introduced in place of the natural sequence encompassing the position of the imprint. The six PstI substitutions scan the imprinted sequence by steps of 1 nucleotide. In these strains, the level and position of the imprint were identical, demonstrating that the imprint is site specific but sequence independent (86), a result independently confirmed (87). Recently, the position of the imprint has been found by chromatin immunoprecipitation coupled with sequencing (ChIP-Seq) (Fig. 4E). The experimental conditions used for ChIP-Seq sequentially include formaldehyde fixation followed by chromatin sonication. The sheared chromatin can be used either before or after immunoprecipitation of chromatin-associated proteins for Illumina library preparation and sequencing. This method retains the first nucleotide of the 5' ends of all sonicated DNA fragments. The abundance of DNA fragments initiating at the position of the imprint was striking (88). Furthermore, the beforehand fixation of the cells with formaldehyde should prevent the accidental cleavage of the imprinted strand by an RNase, and the absence of missing bases under these conditions supports the "nick" model, whereby sonication preferentially breaks, in a window of 10 to 15 nucleotides, the intact strand facing the strand that is nicked. More recently, new approaches have been published to map single-strand DNA breaks at the nucleotide resolution level in bacteria, yeast species, and humans (89–91).

The imprint is assumed to be the initiating event of MTS, indicating that the switching pattern is dictated by both the formation and maintenance of the imprint, which, in turn, trigger the process that replaces the preexisting *mat1* allele with the alternative allele. Next, researchers attempted to separate the steps involved in imprinting and MTS and to identify *trans*-acting factors as well as *cis*-acting elements required for one or the other event.

THE IMPRINT IS MADE DURING *MAT1* DNA REPLICATION

An important insight into the process of imprinting came with the discovery that the polarity of DNA replication is critical for the proper establishment of the imprint and the subsequent MTS process. By analyzing the presence of the imprint in synchronized cultures, using the cautious agarose plug extraction approach, the broken *mat1* centromere-distal DNA fragment was detected during S phase. This result indicates that the replication fork arrives from the centromere-distal side of *mat1* to merge with the imprint and form a polar DSB (82). Two-dimensional (2D) gel electrophoresis, a dedicated method for studying the replication fork progression, subsequently revealed that the polarity of DNA replication at *mat1* is established by a strong *mat1*-distal DNA replication origin (92–94) (Fig. 4C). This polar replication orientation is reinforced on the other side by the *mat1*-proximal replication termination site 1 (RTS1), which prevents any replication fork arriving from the opposite direction to proceed. RTS1 is located about 1 kb centromere proximal of *mat1* and has been restricted to an 800-bp EcoRI fragment (Fig. 4A) (95). The deletion of the RTS1 element has only a small impact on the formation of the imprint and MTS and probably evolved to optimize the process. This structural organization compels *mat1* to be replicated in a single direction, ultimately to position the *mat1*-distal replication pause site 1 (MPS1) in an active configuration for the formation of the imprint (Fig. 4A) (82, 93, 94).

The characterization of the *trans*-acting switching factors *Swi1*, *Swi3*, and *Swi7* has provided essential information on the imprinting process required for MTS (96). *Swi1*

and Swi3 are similar to Tof1/TIMELESS and Csm3/TIPIN in *S. cerevisiae*/mammals. This fork protection/progression complex (FPC) is well conserved across species and includes Swi1 and Swi3 as well as Mrc1/CLASPIN, which also participates in the activity of MPS1 and travels with the replication fork to coordinate progression of the DNA polymerases with that of the replicative helicases (MCM), stabilizing the fork upon fork stalling (97–99). In the absence of Swi1p or Swi3p, the intensity of the pause at MPS1 and of the DSB/imprint is drastically reduced (Fig. 4B to E). *Swi7* encodes the catalytic subunit of DNA polymerase α essential for priming Okazaki fragments at the replication origins and on lagging strands (93, 100). However, pausing and breaking can be dissociated, since in the *swi7-1* ($\text{Pol}\alpha$) mutant, MPS1 is fully active while the DSB/imprint is barely observed. The replication polarity of *mat1* allows putting forth a working model in which Swi1/3 stabilizes the replication fork pause at MPS1 in a region that encompasses the imprinted sequence. This step is followed by Swi7-dependent replication restart and imprinting that support the idea that the imprint is an RNA primer synthesized by the $\text{Pol}\alpha$ -associated primase, responsible for the initiation of Okazaki fragments at replication origins and for lagging-strand synthesis. The ligation of a precisely but partially processed Okazaki fragment will generate the DNA-RNA-DNA intermediate proposed to be the imprint at *mat1* (83, 87).

A recent article from the Singh laboratory challenges the direct implication of the $\text{Pol}\alpha$ primase subunit and proposes instead that the minichromosome maintenance protein 10 (Mcm10) essential for proliferation is a new imprinting enzyme that inserts ribonucleotides at the site of the imprint (101). This view is supported by a primase activity carried by Mcm10, although this activity has been reported only in fission yeast (101, 102). Mcm10 is present at the replication origin to promote initiation of DNA replication by recruiting $\text{Pol}\alpha$ and facilitating Okazaki fragment synthesis in many eukaryotic systems. Mcm10 also functions during replisome elongation, coordinating the progression of the replicative helicases with several proteins present at the replication fork, including $\text{Pol}\alpha$ and the Swi1-Swi3 complex (for a recent review, see reference 103). In addition, Mcm10 also interacts physically and genetically with homologous recombination (HR) proteins (104, 105) present at replication fork barriers (see below). Finally, the genetic interaction between *mcm10* mutants and *swi1*, *swi3*, or *swi7* mutants shows that the double mutants exhibit a cumulative reduction of MTS in comparison to the individual mutants, suggesting that Mcm10 functions possibly at the crossroad of the pause at MPS1, replication restart, and imprinting.

Additional evidence for imprinting during DNA replication was obtained by constructing an inducible MTS strain. The *nmt1* (no message in thiamine 1) promoter was introduced upstream of *mat1* to force transcription through the imprinted DNA strand. This setup resulted in the loss of the imprint and the elimination of MTS by freezing a cell population with unswitchable alleles at *mat1* (*Mu* or *Pu*) in a reversible manner. This system accumulates more M than P cells (see below). A population containing a transcription-dependent stabilized *mat1-M* (*Mu*) has been synchronized. The addition of thiamine to the medium rapidly represses the transcription from the *nmt1* promoter, restoring all functional properties of MTS and allowing the sequential monitoring of the MTS steps on a synchronized cell population. The replication fork pausing at MPS1 is associated with Swi1 accumulation and formation of the site- and strand-specific imprint during the first round of DNA replication, which remains stable for the rest of the cell cycle. It is only during the second round of DNA replication that “one-fourth” of the *mat1-M* allele switches to the P allele. In this molecular pedigree, two consecutive asymmetric cell divisions are necessary to produce one mating-type-switched cell among four related cousins, recapitulating the “one-in-four” switching rule. It also shows that the process is effective not only under starvation conditions but also during vegetative growth (106). To summarize, imprinting occurs on the newly synthesized lagging strand and will generate a one-ended DSB during the following round of DNA replication (see below in Fig. 6). At this time, we do not know where and when Mcm10 plays a role, and future work is necessary to clarify its function in MTS.

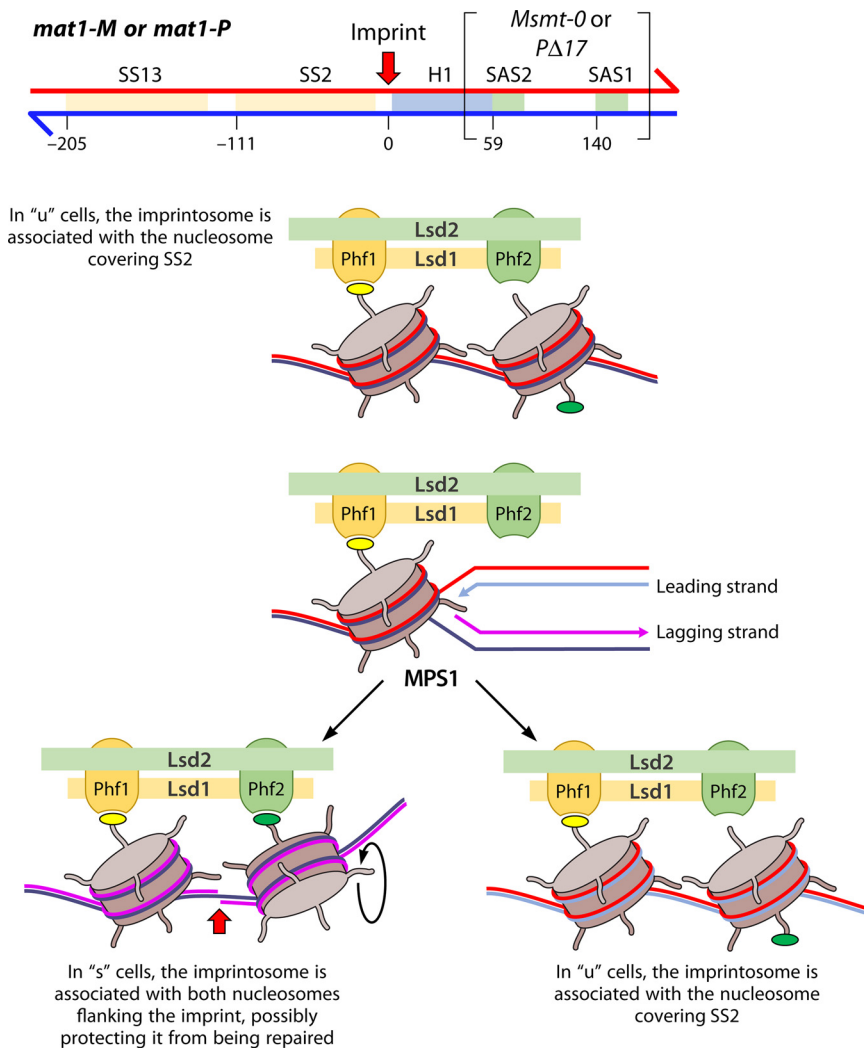


FIG 5 Imprintosome model at *mat1*. The position of the *cis*-acting elements flanking the imprinted site (red arrow) is indicated. In "u" cells, the nucleosome reader Phf1 is associated with a nucleosome that overlaps the SS2 region. During S phase, the imprintosome pauses the fork at MPS1. Following imprinting, the imprintosome establishes a new contact with the nucleosome on the other side of the imprint via Phf2 in "s" cells. The new distal DNA overlaps a region important for imprint stability. Here, the imprint is represented as a nick that allows the free rotation of the nucleosomes. The green and yellow lollipop represent histone modifications recognized by Phf1 and Phf2.

CIS- AND TRANS-ACTING ELEMENTS REQUIRED FOR PAUSING AND IMPRINTING

The initial strategy to identify *cis*-acting elements for imprinting was to analyze the sequence flanking *mat1*, because M and P sequences are different and neither *mat2-P* nor *mat3-M* is cleaved *in vivo*. The first series of deletion mutants on the centromere-distal side of *mat1* identified the switch-activating sites 1 and 2 (SAS1 and SAS2), located at 140 bp and 59 bp to the right of *mat1*, respectively (Fig. 5). Each deletion leads to a reduced rate of MTS and imprinting (54, 62, 65). When mutations in the *cis*-acting SAS1 or SAS2 are combined with the trans-acting *swi1*, *swi3*, or *swi7* mutants, the resulting strains exhibit a cumulative defect in MTS, suggesting that these proteins do not function on the sequences defined by these sites. Larger deletions called *mat1-Msm1-0* and *mat1-P Δ 17* (Fig. 5) encompassing the SAS1/2 sites exhibit a wild-type level of pausing at MPS1 but lack the imprint, making stable M or P cell populations (heterothallic) (54, 107). This result is consistent with the absence of DSBs in the heterothallic *h⁺* variant that fuses the *mat1-P* cassette with the *mat2-P* cassette, generating the *mat1-P:2* cassette while removing the SAS1/SAS2 sequences. ChIP has indicated that

Swi1p is enriched at MPS1 during S phase regardless of the presence of the imprint and is consistent with its association with the replication fork at the arrested and stabilized replisome (106). A more precise analysis using short substitution mutations, called *mut*, within the H1 repeat has identified two types of elements; *mut3* participates in MPS1 activity, whereas *mut5* and *mut7*, which affect neither pausing at MPS1 nor imprinting during S phase, are necessary later in the process to protect the imprint from being repaired/removed during the cell cycle progression, resulting in a steady-state reduction of MTS (108). More recently, Southern blot analysis of synchronized *mat1-Msmt-0* strains revealed a transient DSB at *mat1* during replication that is rapidly and fully repaired during the following G₂ phase, hence resulting in a stable M cell population (unpublished result). Collectively, it was concluded that the centromere-distal side of *mat1* (H1, SAS1, and SAS2) participates mainly in the process that protects the imprint from being erased, consistent with the idea that the imprint is made during S phase, licensing the chromatid for MTS for the following replication round.

Since the sequences outside the *mat1* cassette are not involved in the replication fork pausing activity at MPS1 and imprinting, the sequences within the M and P alleles as well as downstream of MPS1 have been investigated (87). The *SS2* element is located in *mat1-M* within the centromere-proximal 111 bp from the broken site (imprint) in H1 and is required for both MPS1 activity and imprinting. The *SS13* element is located within the 205 bp further inside *mat1-M* and is important for imprinting, while only mildly interfering with MPS1 activity (Fig. 5). The *SS13* deletion exhibits a phenotype similar to that of *mat1-Msmt-0* and *mat1-PΔ17*, but instead of protecting the imprint from repair, it has been proposed to act directly on its formation. The replacement of the *SS13* sequences by a random sequence restores the imprint almost completely, suggesting that this region acts as a spacer element separating functional elements important for imprinting. However, deletions further away from the imprinted site and affecting the *mat1-Mc* coding or promoter regions did not provide any insight into the process of imprinting. Nonetheless, *SS13* has been proposed to influence the positioning of the Okazaki fragment within the *mat1* cassette, approximately 350 nucleotides away from the position of the imprint during the release from MPS1. The model suggested that the one or two ribonucleotides forming the imprint are provided by a partial processing of the next Okazaki fragment (see the model in reference 109). The replication pause site at MPS1 was also observed at *mat1-P*, and although the region corresponding to *SS13* and *SS2* lacks sequence similarity, the deletion of the corresponding segments affects MPS1 and imprinting activities of *mat1-P* as well. Interestingly, MPS1 is active only at the *mat1* cassette and not at the silent *mat2-P* and *mat3-M* cassettes, although *mat3-M* is replicated early and with the same polarity as *mat1*. On the other hand, *mat2-P* is replicated mainly in the opposite direction (87, 110). At least for the *mat2-P* donor, the fork polarity is not sufficient to trigger the pausing activity at MPS1.

In a search for new mutants involved in imprinting, the thiamine-inducible MTS strain was converted into a conditional strain in an HR mutant (*rad51Δ*) background (111). In this system, cell viability depends on the absence of an imprint at *mat1*, allowing selection for spontaneous viable mutants affected in the MPS1 pause and/or the formation of the imprint. In addition to many new *swi1/3* alleles, we also isolated a new switching mutant in the lysine-specific demethylase 1 gene. Lsd1 is highly conserved and was studied mainly for its role in gene expression (reviewed in reference 112). In fission yeast, Lsd1 is found within a complex with Lsd2 together with Phf1/Phf2. Lsd2 and Phf1/Phf2 are essential for viability, and Phf1/Phf2 contain a plant homeodomain finger that binds to histone marks according to their methylation status (113–115). In humans, a similar association between LSD1 and PHF21A has been described (116). Both Lsd1 and Lsd2 contain an HMG domain in their C terminus that binds A-type DNA, a domain missing in the mammalian counterparts. However, the mammalian proteins interact with the HMG20a/b proteins (111) reported to interact with BRCA2 in humans (117). In fission yeast, the Lsd1 complex interacts with the DNA replication machinery, the switch-activating protein 1 (Sap1), topoisomerase 2 (Top2), and replication protein A (Ssb1) (113). In mammals, LSD1 interacts with the MCM helicases, replication factor C (Rfc), and PCNA (118). In fission yeast, the Lsd1/2

activities prevent H3K9 methylation at heterochromatin boundaries and telomeric regions and were also found enriched on highly expressed genes (88, 113, 114, 119). Lsd2, Phf1, and Phf2 are essential, but the *lsd1*Δ strain is viable and exhibits strongly reduced proliferation (120). However, the demethylase dead alleles of Lsd1/2 (single or combined) remain viable, and the double mutant strain exhibits a reduced pausing activity at MPS1 independently of Clr4, the sole H3K9 methyltransferase in fission yeast, indicating that the methylation of H3K9 is required neither for viability nor for pausing at MPS1 (88, 111). The *lsd1* mutation affecting MTS was found in the HMG domain and decreases the level of Lsd2 protein, thus reducing the overall Lsd1/Lsd2 activity. Evidence for a direct role at MPS1 of both proteins was provided by their enrichment at *mat1-M* and *mat1-P* and not at the silent *mat2-P* and *mat3-M* loci (88, 111). Furthermore, the binding of Lsd1 to *mat1-M* is lost in the *SS2* deletion, not affected by *SS13* or *Msm1-0* deletions, and not impacted by the absence of Swi1 or Swi3. Thus, the main conclusion for Lsd1 and Lsd2 is that they work redundantly and upstream of Swi1/3 to arrest the fork at MPS1. Neither the enrichment of Lsd1/2 at different sequences in *mat1-M* and *mat1-P* nor the lack of enrichment of Lsd1/2 at the homologous silent cassettes depends on H3K9 methylation, since a similar distribution of Lsd1/2 is observed in the absence of Clr4. It is not the DNA sequence at the *mat1-M* or *mat1-P* allele that is recognized by the Lsd1/2 complex. Instead, it was proposed that the Phf1/Phf2 histone code readers direct Lsd1/2 to *mat1* (Fig. 5) as well as to actively transcribed genes. Sap1 binds the SAS1 and SS13 elements and is involved in the replication fork barrier (RFB) at the ribosomal DNA (rDNA) and the replication fork pause at the Tf2 transposons (121, 122). The physical interaction of Lsd1 with Sap1 suggests another mode of recruitment at least to *mat1-M*. The situation is not as clear at *mat1-P*, where Sap1 was not found enriched inside the P allele (88).

The sonication applied during the ChIP experiments described above generates a precise and unique sequencing signature at the 5' end of the imprint, exactly at the position previously mapped by molecular approaches (74). Although Lsd1/2 was found enriched at SS2 regardless of the presence of the imprint (in *h⁹⁰*, *h⁹⁰ swi1*Δ, and *mat1-Msm1-0* backgrounds), it was also found associated with DNA on the distal side of the imprint, containing the H1 sequences with the 5' end of the imprint. Thus, it was proposed that the Lsd1/2 complex interacts with both sides of the imprint. The binding to SS2 promotes the pause at MPS1 prior to imprinting. Following imprinting, the Lsd1/Lsd2 complex also binds the other side of the imprint, potentially protecting it from DNA repair. This large nucleoprotein structure was called the "imprintosome" (123, 124). In the model shown in Fig. 5, we propose that Phf1/Phf2 provide the anchor recruiting the imprintosome facilitated by the free rotation of the DNA around the imprint, shown as a single-strand break (SSB). The imprintosome is involved during each replication round to establish the imprint on the lagging strand in the presence or absence of the *mat2/mat3* cassettes (79, 80, 88).

OTHER REPLICATION FORK BARRIERS

DNA replication and recombination have been holding hands for a long time and have brought answers to many different needs during evolution. The studies of replication pausing at programmed replication fork barriers highlighted common features concerning the mechanisms of replication restart. However, the growing number of publications reporting new examples of fork barriers or pauses involved in various biological roles taught us to be cautious in overgeneralizing the conclusions reached on one type of replication fork barrier (reviewed in reference 125). In fission yeast, Swi1p and Swi3p as well as Lsd1/2 are required to enforce MPS1 and RTS1 at *mat1* and RFB at rDNA (111, 131, 132). Sequence-specific DNA-binding proteins have also been implicated in programmed replication fork barriers, among which are Rtf1 at RTS1, Sap1 and Reb1 at RFB, and Sap1 at long terminal repeats (LTRs) (88, 95, 121, 122, 126). A role for Sap1 at MPS1 was supported by introducing SAS1 on plasmids (127), but so far, its function in MPS1 activity remains elusive.

The blockage of the fork is withdrawn by removing the bound protein using

specialized DNA helicases (128–130) or by a replication fork moving in from the other side. In response to a persisting block, the unbroken replisome can be dismantled while the DNA can be stabilized by forming a reversed fork with a four-way junction commonly called “chicken foot.” The annealed nascent DNA strands form a one-ended DSB that recruits the HR machinery. Interestingly, RTS1 becomes recombinogenic and loses its regulation by Lsd1 when placed ectopically, suggesting that Lsd1/2 is working at a distance from SS2 on RTS1 and suggesting that Lsd1 could prevent chicken foot formation or single-stranded DNA at stressed replication forks (111, 131, 132). For instance, failure to pause at MPS1 in Lsd1 mutants allows the fork incoming from *mat1* to replicate across RTS1, thus abolishing its function. Despite the rapid recruitment of Rad52 (previously called Rad22 in fission yeast) only at RTS1 located at ectopic sites, cell viability is not affected in its absence, suggesting that other processes, such as the timely arrival of a replication fork from the opposite side prior to any pathological consequence, are involved (131–133). Recovery of stalled forks at RTS1 has been described without an associated DSB and was named recombination-dependent replication (RDR) (134–136). A similar situation as the RDR has been reported in budding yeast and mouse cells using the prokaryotic Tus/Ter replication barrier (137).

The break-induced replication (BIR) process is in many aspects similar to RDR but has been studied almost exclusively during the G₂ phase of the cell cycle in the context of a DSB. More recently, BIR was examined during DNA replication when the fork is running into a site-specific nick that generates a one-ended DSB (138). In both RDR and BIR, completion of DNA replication is not performed by the canonical replisome machinery, and DNA synthesis of the unreplicated region is either semiconservative (RDR) or conservative (BIR). The two complementary strands are made sequentially by two runs of DNA polymerase delta that uncouple leading- and lagging-strand DNA synthesis (139, 140). Under these conditions, the fidelity of DNA synthesis and sister chromatid cohesion as well as the correct redistribution of new and parental histones might be compromised (136, 141). In mammals, common fragile sites or telomeres are duplicated very late, with DNA synthesis still occurring during G₂ or early mitosis. These processes are highly recombinogenic and named MiDAS and ALT, respectively. These events are reminiscent of BIR studied in the context of replication over a “nick” or in the G₂ phase and require the recombination proteins Rad51, Rad52, and Rad54 along with helicases and the structure-specific nuclease Mus81 (142).

MATING-TYPE SWITCHING PROCESS

The imprint creates a single-strand discontinuity in the DNA duplex at *mat1* that triggers MTS. In both the “nick” and ribonucleotide models, the imprint was proposed to be converted into a replicative polar or one-ended DSB upon the passage of the leading-strand DNA polymerase, restricting MTS to only one of the two sister chromatids (82, 84, 143). Synchronization of the cells in the inducible system indicated that the first DNA replication round establishes the imprint, while the second round generates a polar one-ended DSB that initiates a replication-induced recombination process that replaces the information present at *mat1* with that of the alternative silent allele present either at *mat2* or at *mat3*, leading to *mat1* switching (82, 86, 106). The gene conversion repairs the imprinted strand, whereas an imprint is introduced into the newly synthesized lagging strand, thus sustaining the chain of consecutive switching.

Key recombination proteins involved in the search for homology, such as the MRN (Mre11-Rad50-Nbs1) complex, Rad51, and Rad52, are needed for the repair of broken forks, and HR-deficient mutants produce dead cells in the presence of the imprint regardless of the presence of *mat2/mat3* donors. Because the *mat1-Msmt-0* strain remains fully viable in HR mutants, it was concluded that a single unrepaired imprint generating a one-ended DSB leads to cell death in the absence of HR, emphasizing the importance to normal DNA metabolism of repairing frequent and apparently mild damage. Furthermore, in *mat1-Msmt-0* strains, MPS1 and all the other replication fork

pauses or arrests are fully active; thus, fork reversal is either transient or not formed, and DNA replication resumes without breakage under physiological conditions (80).

Initiation of MTS at the one-ended DSB is supported by several observations. Following the formation of the one-ended DSB, the H1 homology sequence present at the 3' OH end of the break is processed by the MRN complex to form a protruding 3' end that invades one of the H1 sequences of the donor cassettes (Fig. 5). This is consistent with progressive elimination as a function of the distance from the DSB during the conversion process of the linker-scanning PstI substitution mutations introduced upstream of the DSB (86). This result indicates that DNA strand invasion initiates with a limited length of H1 homology (59 bp). Like other HR processes, the nucleoprotein Rad51/H1 filament catalyzes pairing between the H1 element at *mat1* and one of the H1 sequences of the donors to promote strand invasion and form a displacement loop (d-loop) intermediate. The initial d-loop is probably stabilized by the Rad51 mediators (Rad55-Rad57) and the Msh2 protein (Swi8), since mutations in these proteins generate similar substitution mutations near the H1 homology box of *mat1* (80, 144). The substitution is made during aberrant gene conversion and reveals *cis*-acting elements next to the H1 sequence of the *mat1* locus important for imprinting and subsequent MTS (80). Following the stabilization of the invading 3' end and within the d-loop, DNA synthesis can proceed using the opposite mating type as a template. As in the BIR process, DNA synthesis probably uses DNA polymerase delta to reach the H2 sequence on the other side of the donor in 1 or 2 min (145). Using dedicated PCR primers, we captured the gene conversion intermediates that extended beyond the H3 sequence that connects *mat1* to the *mat2* or *mat3* donors (Fig. 6, step f) (143). We do not know how and where the gene conversion tract stops, but the d-loop can progress several kilobases further. This was substantiated by the numerous rearrangements observed in the heterothallic strains that are even more frequent in DNA repair mutants required for the resolution of gene conversion (17). The annealing of the H2 sequence synthesized off the donor with the H2 sequence present at *mat1* can be resolved either by the mismatch repair enzymes Msh2/Msh3, the structure-specific endonuclease complex Rad16/Swi10 initially identified as "swi" genes 4, 8, 9, and 10 and *pxd1*, a platform allowing the concerted activity of Swi9/10 and Dna2 nucleases and homologous to *MSH3*, *MSH2*, *RAD1*, *RAD10*, and *SLX4* in budding yeast (96, 143, 146–150). Rad52 is essential in homothallic strains and in the strains with *mat2/mat3* deleted, exhibiting Rad52-YFP foci associated with a major enrichment at *mat1* during S phase. This is in sharp contrast with the *mat1-Msmt-0* and *mat1-PΔ17* strains that are devoid of foci and enrichment although sustaining a fully active MPS1 (80). Furthermore, the *rad52-67* hypomorphic allele exhibits an MTS resolution defect and produces heterothallic variants, indicating a function during both the imprinting-dependent initiation and subsequent termination steps (146). The resolution process by synthesis-dependent strand annealing (SDSA) is similar to that proposed earlier for *S. cerevisiae* MTS (151, 152). In the migrating d-loop, single-stranded DNA is produced, and the synthesis of the complementary strand is uncoupled, waiting for either the resolution of the gene conversion event or for Pol α (and ligase 1), as proposed for BIR, to initiate the synthesis of the cDNA strand and explain the MTS defect observed in the mutant (153, 154). Using light radioisotopes, we found that both of the newly synthesized DNA strands are found at the switched *mat1* locus, demonstrating a conservative process (143, 155). The parental DNA strand containing the imprint is eliminated during MTS, and a novel imprint is deposited on a newly synthesized DNA strand, indicating that the imprinting process needs to be reiterated at each round of replication. This new imprinted strand can be made by Pol α along with Mcm10 as suggested above but can also be synthesized by the processive DNA polymerase released from fork arrested at RTS1 (see yellow highlighted steps in Fig. 6).

Many of the HR proteins are required for cell viability in strains proficient for imprinting, regardless of the presence of the *mat2/mat3* donor loci. The noticeable exceptions are the structure-specific endonucleases Swi9/Swi10 and Mus81/Eme1. In the presence of the donors, Swi9/Swi10 is dedicated to MTS. In their absence, Mus81/Eme1 becomes essential for survival, but viability can be recovered in the absence of the imprint. It was proposed that the one-ended DSB is repaired by invading the sister

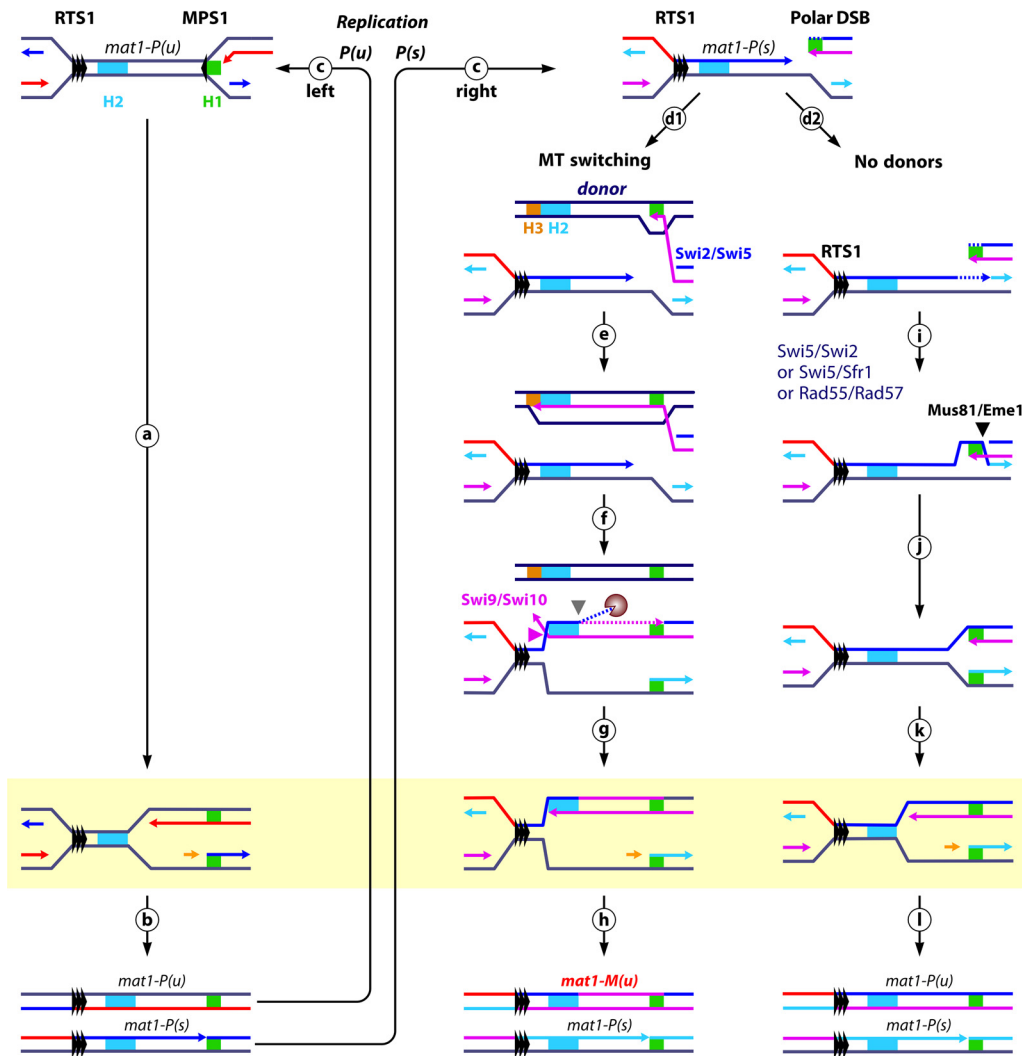


FIG 6 Recombination-dependent replication model. Starting from a virgin *mat1-P(u)* template, the replication forks arrest at *RTS1* and pause at *MPS1*. (a) Site-specific lagging-strand reinitiation (orange arrows), also depicted in steps g and k. (b) Upon replication restart, *mat1-P(u)* and *mat1-P(s)* are generated. (c left) Replication of *mat1-P(u)*. (c right) During the replication of the *mat1-P(s)* template, *RTS1* arrests the replication fork coming in from the left while that coming in from the right converts the SSB into a polar one-ended DSB recognized by the MRN complex. Mre11-dependent 5'-to-3' resection produces a 3' OH overhang. (d1) In the presence of the donors, the 3' overhang uses the *Swi2/Swi5* complex to invade the correct donor sequence, forms a d-loop, and initiates mating-type switching. (e) d-loop extension. (f) Resolution using the *Swi9/Swi10* endonuclease (pink triangle) associated with the mismatch repair machinery (not represented). How the old *mat1* sequence is disposed of is not known, but two scenarios have been proposed (gray triangle, endonuclease; gray "pacman," exonuclease). (g) Site-specific lagging-strand reinitiation. (h) Generation of the switched virgin *mat1-M(u)* allele and reengineering of the *mat1-P(s)* allele. (d2) In the absence of donors, the 3' overhang invades the replicated sister chromatid. (i) Strand invasion and d-loop formation require the *Swi2/Swi5*, *Swi5/Sfr1*, and *Rhp55/Rhp57* complexes. (j) The d-loop is next resolved by the *Mus81/Eme1* complex (black triangle) that resets a replication fork with no strand exchange. (k) Site-specific lagging-strand reinitiation. (l) Generation of *mat1-M(u)* and reintroduction of the imprint at *mat1-P(s)*. The yellow shading highlights the fact that all three intermediates generating the imprint produce the same outcome.

chromatid to form a d-loop, which is subsequently converted into a replication fork by *Mus81* (Fig. 6). Consequently, in the absence of both the donors and *Mus81*, cells that inherit the imprint die while cells that inherit the virgin chromatid survive and generate a linear growth that can be observed in a pedigree (80). A similar role for *Mus81* was recently reported using an artificial system creating a long-lived nick that can be converted into a broken fork during DNA replication and allowing the study of BIR in the context of S phase (138). In the ribonucleotide model, a role for the flap endonuclease *Fen1* (*S. pombe* *Rad2*), RNase H1/H2, topoisomerase 1, or tyrosyl-DNA

phosphodiesterase in the process of repair by ribonucleotide excision has been proposed. These enzymes are, therefore, good candidates for the cleaving or processing of the imprinted strand (156–158). However, *rad2Δ*, *rnh1-201Δ*, *top1Δ*, or *tdp1Δ* mutant strains are fully proficient in MTS (47, 93, 159, 160), and additional studies are required to gain a more precise understanding of the molecular nature associated with the formation and processing of the unusual type of imprint used for MTS in fission yeast. This replication-dependent recombination event has been genetically strengthened by showing, on the one hand, the formation of heteroduplex DNA during the initial strand invasion that forms a d-loop at the H1 homology box of one of the donor cassettes and, on the other hand, d-loop migration coupled with DNA synthesis and gene conversion resolution at the respective H2/H3 homology boxes without any crossing over (80, 108, 144, 161).

ESTABLISHMENT AND MAINTENANCE OF HETEROCHROMATIN AT THE MAT2/MAT3 REGIONS

The choice between the two donors is the second aspect central to MTS that relies on the actors involved in the silencing mechanism of the *mat2/mat3* region. Heterochromatin is a tightly packed form of chromosomal DNA that is poorly expressed. This organization comes with flavors ranging from constitutive to facultative heterochromatin, depending on their establishment and maintenance modes. Apart from access to DNA sequence information, histone modifications recruit proteins that assemble higher-order chromatin structures critical for heterochromatin functions. Counterintuitively, transcription of the *dg* and *dh* satellite repeats of the K region is required for silencing (162). These noncoding RNAs are processed by the RNA interference (RNAi) machinery, including argonaute, dicer, and an RNA-dependent RNA polymerase (RdRP), into small interfering RNAs (siRNAs) that are essential for *de novo* formation of the constitutive heterochromatin (163–165). The siRNA provides the guide to target the Clr4 methyltransferase to the satellite repeats for histone H3K9 methylation, providing a platform recruiting the heterochromatin protein 1 (HP1) homolog, Swi6 (63, 166–170). Swi6 is used as a platform for the histone remodeler and deacetylase complex SHREC, which contains the Rik1, Clr1, Clr2, Clr3, and Mit1 proteins involved in chromatin silencing (171, 172). Recently, the *S. pombe* AP1-like factor Pap1 was reported to be recruited to *cenH* and to participate in silencing (173, 174). The two other important silencing elements, REII and REIII, recruit histone deacetylases (Clr3, -5, and -6) and the NAD-dependent deacetylase Sir2, allowing the subsequent H3K9 methylation and Swi6 spreading (175–177). REII works through Clr5, and REIII contains binding sites for the stress transcription factors Atf1/Pcr1 (Fig. 4A). The latter (refers to REIII) recruits the histone deacetylases Clr3 and Clr6, enabling H3K9 methylation and Swi6 recruitment independently of the RNAi process (67, 73, 178, 179). Atf1 was proposed to promote facultative heterochromatin formation in a context-dependent manner, globally increasing phenotypic plasticity (180). Recently, ORC proteins and the DNA-binding protein Deb1 have been found associated and working with REIII. The REIII binding factors improve the maintenance of silencing probably by promoting the recruitment of Clr4, Rik1, and Raf1, which are part of the CLRC complex (73, 181) that is linked to the replication fork (182). The Sir2 deacetylase is required for removing the acetyl group on H4K16, thus facilitating methylation of H3K9 and heterochromatin spreading (183). Finally, stable epigenetic inheritance, independent of RNAi, requires the Epe1 antisilencing factor, a member of the Jumonji demethylase family (63, 184, 185).

The silent region is framed by two boundary elements made of the 2-kb inverted repeats IR-L and IR-R (71, 72) (Fig. 4A and 7). Both repeats are bound by Sap1 (88) and are at the transition between heterochromatin (H3K9me and Swi6) and euchromatin modifications (H3K4me). Boundary elements counteract the intrinsic properties of the different chromatin domains to extend into the neighboring sequences. In this context, it has been proposed that a boundary requires the combination of two histone H3 demethylase enzymes, including the JmjC domain protein Lid2 acting on H3K4 and the lysine-specific demethylases (Lsd1/2) acting on H3K9 (113, 119).

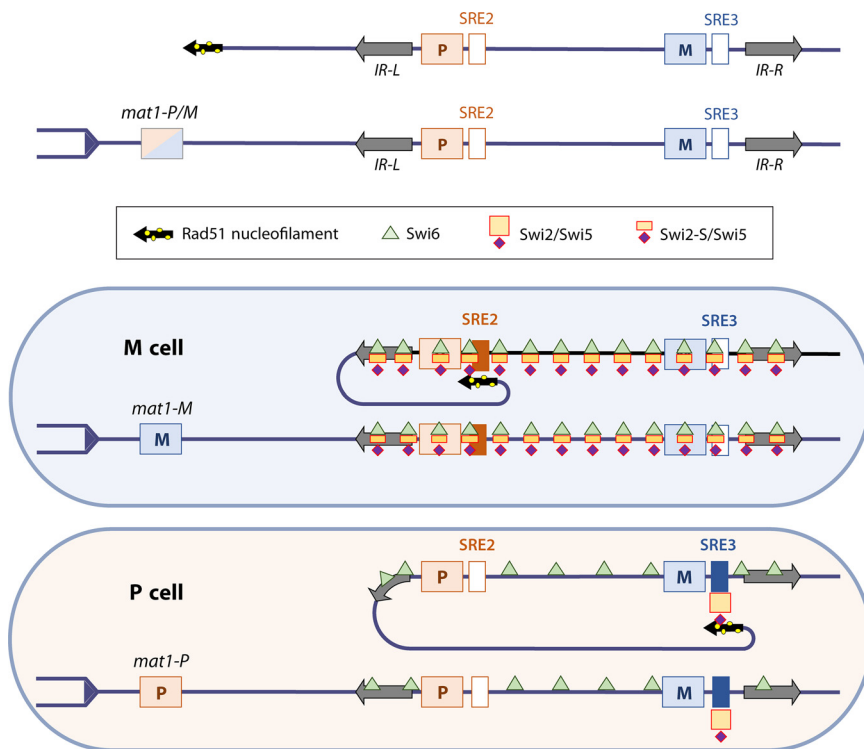


FIG 7 Directionality of switching model. Two Swi2/Swi5 recombination enhancers are located next to H1 of *mat2* (SRE2) and *mat3* (SRE3). The expression of the M or P allele at *mat1* triggers different properties of the two enhancers. In M cells, the Mc transcription factor and the CENP-B homolog Abp1 bind to the *swi2* locus to activate an alternative promoter, producing a shorter Swi2 variant (Swi2-S). The Swi2-S/Swi5 complex covers the entire *mat2/mat3* region, licensing SRE2 in M cells in a Swi6-dependent manner. In P cells, the Swi2/Swi5 complex is enriched independently of Swi6 only at SRE3.

Each repeat contains B-box sequences bound by the TFIIIC complex present at polymerase III promoters and organizing chromosomal domains at the nuclear periphery (71). The RISC complex associates with TFIIIC and spreads on H3K9me-Swi6 chromatin to tether the K region to the nuclear envelope via the nuclear rim protein Amo1. Amo1 works through the interaction with the Pob3 and Spt16 subunits of FACT, in a pathway similar to that of the Fun30 chromatin remodeler Fft3, indicating that histone turnover is required for boundary function (72, 186, 187). Sap1 is also enriched on both inverted repeats and may participate in chromosome organization (54, 88, 122, 188, 189). The implication of TFIIIC in recruiting condensin at the B box and the role of Sap1 in chromosome condensation could contribute to a robust, highly folded heterochromatin *mat2/mat3* region promoting an optimum configuration for MTS (187, 189–191). Finally, several reports have indicated that DNA replication and silencing work together. Autonomously replicating sequences (ARS) are functionally associated with DNA elements important for repression, and Swi6 activates replication origins at pericentromeric and *mat2/mat3* regions (192, 193). Factors of the replisome, including Mrc1/Claspin, Mcl1/Ctf4/Swi1/Timeless, Asf1/HIRA, Pob3/FACT, and Fft3/SMARCAD as well as the DNA polymerase epsilon-interacting proteins Dos1/Clr8, Dos2/Clr7, Rik1, and Lid2, have been proposed to guide nucleosome assembly and maintain modified histones at their place at each round of DNA replication (182, 194–196). Genome-wide mapping approaches have indicated that *dg/dh* transcription is transient during S phase (197, 198), potentially spreading heterochromatin with the replication fork (182, 199). The sequence homology of several noncoding sequences indicates functional constraints. For the H1 and H2 boxes, the homology is involved in base pairing for the initiation and resolution of the MTS process (see below). For the *cenH* sequence, it is still difficult to distinguish whether it is acting in *trans* by borrowing siRNA made from the centromeric sequence and/or in *cis* by using transcripts of the K region. The 2-kb-long

perfect homology of the repeats suggests direct DNA base pairing between them, forming an unusual Watson-with-Watson and Crick-with-Crick pairing (200). It is possible that IR-L/IR-R are relics of the inverted repeats used in a HR-directed process named flip/flop that is frequently described for MTS in budding yeast species (201). Among many natural isolates, only a single orientation of the mating-type cassettes has been reported (18), indicating that strand exchange between IR-L/IR-R repeats are rare or nonexistent. Collectively, these results indicate that the *mat2/mat3* silent region combines redundant constitutive heterochromatin and facultative heterochromatin, which collaborate in histone modifications and nucleosome repositioning to ensure transcription silencing and global DNA recombination repression, ultimately allowing a higher order of chromatin organization that is instrumental in the process that controls the directionality of MTS (195, 202).

TWO DONORS' CHOICE: DIRECTIONALITY OF SWITCHING

The process of MTS observed in haploid and diploid cell pedigrees is highly efficient (4, 49), supporting a dedicated mechanism for donor choice called directionality of switching (52). Directionality refers to a nonrandom choice of the cassette used to repair the broken replication fork at *mat1*. In other words, in M cells, the one-ended DSB containing the H1 homology box of *mat1-M* is directed to the H1 sequence of the *mat2-P* cassette, whereas in P cells, it is directed to *mat3-M*. The initial experiment of swapping the P and M sequences between the H2 and H1 homology boxes of the silenced donors showed a drastic reduction of MTS, from 90% in *h⁹⁰* to nearly 9% in the swapped cassette strain (therefore called *h⁰⁹*). This result indicates that the allele expressed at *mat1* directs a chromosomal folding that favors the choice of the donor locus regardless of its content to facilitate recombination, indicating that *cis*-acting elements located outside the silent cassettes are responding to the MT of the cell (171). The *swi2*, *swi5*, and *swi6* "switching" mutants, which exhibit a wild-type level of imprinting but a low switching efficiency (203), have been instrumental in elucidating how heterochromatin, traditionally hostile to mitotic and meiotic recombination, can promote site-specific gene conversion to support the directionality of switching. The absence of the chromodomain protein Swi6 has opposite effects on MTS in the *h⁹⁰* and *h⁰⁹* strains, decreasing switching in *h⁹⁰* and increasing it in *h⁰⁹*. Similar results have been obtained with mutants in the pathway of H3K9 methylation (Sir2, Clr3, Clr4, Clr7, Clr8, and Pcu4) (52, 166, 194, 204–206). Twenty genes, including those coding for proteins of the Set1 complex implicated in H3K4 methylation and Brl2 involved in H2BK119 ubiquitination, have recently been added to this list, with only little information concerning their function (57).

A central argument for a directionality default is the bias found in the ratio of M and P cells in a clonal population. In this context, the *h⁹⁰ swi6* mutant strain is biased toward M cells, indicating that *mat2-P* is used relatively less efficiently than *mat3-M*. Conversely, *h⁰⁹ swi6* mutants are dominated by P cells, consistent with the poor usage of *mat2-M*. This result implies a role for Swi6 in favoring the use of the *mat2* locus, regardless of the information present (52). Otherwise, as discussed above, the unbroken *mat1* allele carried by the sister chromatid is an alternative template for DSB repair when the donor locus is not available (80).

Swi5 is found in a complex with Sfr1, with which it forms a mediator of the HR protein Rad51 in a pathway parallel to that of Rad55/Rad57, the other mediator complex. Both mediator complexes are required during mitotic and meiotic DNA recombination (207–209). Swi5 is also found in a second and less abundant complex with Swi2 that directly interacts with Swi6 and Rad51. By analogy with Swi5/Sfr1, it has been proposed that Swi2/Swi5 captures the Rad51/H1 nucleoprotein filament and searches for the H1 homology box of the silent cassettes surrounded by Swi6 (207). The functional study of the DNA sequences close to the H1 boxes of the donors made it possible to discover two Swi2/5 recombination enhancers, SRE2 located next to H1 of *mat2* and SRE3 next to H1 of *mat3* (Fig. 4 and 7), which target gene conversion of the respective cassette for MTS (56, 205). The swapping of the SRE elements recapitulates the phenotype of swapping M and P donors as in the *h⁰⁹*

strains, while the double swap (SREs and M and P donors) restores the directionality of the wild-type configuration (56). The expression of the M or P allele at *mat1* makes it possible to distinguish the different properties of the two enhancers. In P cells, Swi2 is enriched independently of Swi6 only at SRE3, possibly via its AT-hook motif. In M cells, the Mc transcription factor and the CENP-B homolog Abp1 bind to the *swi2* locus to activate an alternative promoter, producing a shorter Swi2 variant (Swi2-S) (210–212). Furthermore, *swi2-S* and *swi5* are transcriptionally induced, and Swi6 appears more abundant in the *mat2/mat3* region (211, 213). As a consequence, the Swi2-S/Swi5 complex covers the entire *mat2/mat3* region, licensing SRE2 in M cells in a Swi6-dependent manner (56, 205) (Fig. 7). These observations support the MT bias previously observed in the absence of *swi6* in both the h^{90} (M > P) and the h^{99} (M < P) configurations, since only SRE3 remains active. Combinations of swapped or duplicated SREs in *swi2*, *swi5*, or *swi6* mutant backgrounds further support this model and provide a detailed example of how a cell type identity can differentiate using heterochromatin, which is naturally refractory to recombination (for review, see reference 214). It also provides an explanation for the M > P bias observed in the MTS-inducible system, in which the transcript coming from the *nmt1* promoter could limit Mc expression and favor Swi2 and SRE3. Thus, directionality works in two steps that go against the classic HR dogma, i.e., the search for DNA homology and the refractory nature of heterochromatin. The first step is the physical search for the Swi2/Swi5 mediator complex-coated SRE2 or SRE3 elements with the resected single-stranded DNA covered with Rad51 (nucleofilament containing the DSB). This initial search is favored by the physical proximity of the partners that are constrained by molecular interactions between functional elements of the *mat2/mat3* region at the centromeric periphery and the nuclear envelope. It is only later, when the cassettes are placed near one another, that the second step triggers the Rad51 and mediator proteins to form the d-loop using the DNA sequence homology of the H1 elements, setting the initial structure for gene conversion.

Future studies are needed to shed light on some areas of directionality that are still poorly defined. For example, while both Swi2 isoforms interact with Swi6, it is not clear why Swi2-S spans the silent region while the full-length Swi2 does not. Moreover, how Swi2-S is used selectively on SRE2 while it is also present on SRE3 even when the two SREs are swapped remains an open question. Next, following DNA replication and MTS, the cell enters a long G₂ phase with two polymorphic sister chromatids containing *mat1-P* and *mat1-M*. Hence, *mat1* (M or P) is no longer by itself responsible for the cell identity, leaving the cell with an uncertain gender that might interfere with *swi2/swi5* expression and possibly donor choice. It is possible that the newly converted allele remains transiently silent until mitosis occurs, i.e., inheriting half of the H3K9me3 histones from the silent cassette. Another possibility is that the Swi2/Swi5 and Swi2-S/Swi5 complexes remain at their respective SRE element until mitosis or cell division. A Swi5-dependent bias in gene conversion has been proposed previously in meiosis. This *mat* bias uses the histone deacetylases *clr6* and *hos2* and was observed only in zygotic crosses, when mating is immediately followed by meiosis. The MT bias is lost in an azygotic meiosis, when the M/P diploid cell is allowed to make a few divisions prior to undergoing meiosis, which homogenizes the chromatids and erases the epigenetic memory (215).

CONCLUDING REMARKS

The originality of the approaches and the formalism of the genetic questions applied to biological principles on MTS in *S. pombe* are essentially attributed to Amar Klar, who sadly passed away in March 2017. He was a pioneer in epigenetics by discovering *Mar1/Sir2* in budding yeast, showing the role of Swi6 in nucleation and spreading of heterochromatin through mitosis and meiosis in fission yeast, and proposing the DNA strand-specific imprinting/segregation model (60). His last discovery led him to extend his model of non-random strand chromatid segregation (216) in the support of the immortal strand theory proposed earlier by John Cairns (217). Today, our level of understanding of MTS and asymmetric cell division in fission yeast has reached great molecular details at the DNA or

chromatin level. However, the molecular nature of the imprint remains an open question. The strong functional conservation of the *swi1*, *swi3*, *swi7*, and *mcm10* genes in eukaryotic DNA replication and the importance of the replication fork in the maintenance of epigenetic marks during MTS have been established, but the precise role in imprinting requires further work. For *Isd1*, the link with MTS with respect to replication fork processing and genome stability has been reported in fission yeast and to some extent in other fission yeast species, including the highly diverged *S. japonicus* (5, 218). The literature in mammals focuses on gene expression and also supports the association of LSD1 with DNA replication, recombination, and DNA repair checkpoint through genetic interactions with the DNA methyltransferase DNMT1, BRCA1/2 interacting protein HMG20a/b, and p53, respectively. How much of the asymmetric epigenetic process learned from haploid fission yeast can be exploited to explain the strand-specific imprinting and biased chromatid segregation in other systems is not known, but it is of importance because it is a key area of today's research on developmental biology. Current questions rely on how these epigenetic marks are put in place initially and how they are recognized in order to segregate them correctly according to the pattern of differentiation in diploid cells (59).

ACKNOWLEDGMENTS

This work was supported by grant ANR-18-CE12-0011 to B.A., by the Pasteur Institute, and by the CNRS.

We thank Stefania Francesconi for her critical reading of the manuscript.

We declare no conflicts of interest.

REFERENCES

- Lindner P. 1893. Schizosaccharomyces pombe sp. nov., a new ferment. Wochenschrift Für Brauerei 10:1298–1300.
- Schønning H. 1895. En ny og ejendommeligt Ascusdannelse hos en Gjærsvamp. Medd Carlsberg Lab 4:77–84.
- Leupold U. 1949. Die Vererbung von Homothallie und Heterothallie bei Schizosaccharomyces pombe. Dissertation. Luno, Copenhagen. <https://www.worldcat.org/fr/title/vererbung-von-homothallie-und-heterothallie-bei-schizosaccharomyces-pombe/oclc/493972531>.
- Miyata H, Miyata M. 1981. Mode of conjugation in homothallic cells of Schizosaccharomyces pombe. J Gen Appl Microbiol 27:365–371. <https://doi.org/10.2323/jgam.27.365>.
- Rhind N, Chen Z, Yassour M, Thompson DA, Haas BJ, Habib N, Wapinski I, Roy S, Lin MF, Heiman DI, Young SK, Furuya K, Guo Y, Pidoux A, Chen HM, Robbertse B, Goldberg JM, Aoki K, Bayne EH, Berlin AM, Desjardins CA, Dobbs E, Dukaj L, Fan L, FitzGerald MG, French C, Gujja S, Hansen K, Keifenheim D, Levin JZ, Mosher RA, Müller CA, Pfiffner J, Priest M, Russ C, Smialowska A, Swoboda P, Sykes SM, Vaughn M, Vengrova S, Yoder R, Zeng Q, Allshire R, Baulcombe D, Birren BW, Brown W, Ekwall K, Kellis M, Leatherwood J, Levin H, et al. 2011. Comparative functional genomics of the fission yeasts. Science 332:930–936. <https://doi.org/10.1126/science.1203357>.
- Leupold U. 1970. Chapter 8 Genetical methods for Schizosaccharomyces pombe. Methods Cell Biol 4:169–177. [https://doi.org/10.1016/S0091-679X\(08\)61754-9](https://doi.org/10.1016/S0091-679X(08)61754-9).
- Gutz H, Heslot H, Leupold U, Loprieno N. 1974. Schizosaccharomyces pombe, p 395–446. In King RC (ed), Handbook of genetics, vol 1. Bacteria, bacteriophages and fungi. Plenum Press, New York, NY.
- Nurse P. 1975. Genetic control of cell size at cell division in yeast. Nature 256:547–551. <https://doi.org/10.1038/256547a0>.
- Mitchison JM, Nurse P. 1985. Growth in cell length in the fission yeast Schizosaccharomyces pombe. J Cell Sci 75:357–376. <https://doi.org/10.1242/jcs.75.1.357>.
- Martin SG, Chang F. 2005. New end take off: regulating cell polarity during the fission yeast cell cycle Cell Cycle 4:1046–1049. <https://doi.org/10.4161/cc.4.8.1853>.
- Koyano T, Konishi M, Martin SG, Ohya Y, Hirata D, Toda T, Kume K. 2015. Casein kinase 1 γ ensures monopolar growth polarity under incomplete DNA replication downstream of Cds1 and calcineurin in fission yeast. Mol Cell Biol 35:1533–1542. <https://doi.org/10.1128/MCB.01465-14>.
- Su SS, Tanaka Y, Samejima I, Tanaka K, Yanagida M. 1996. A nitrogen starvation-induced dormant G0 state in fission yeast: the establishment from uncommitted G1 state and its delay for return to proliferation. J Cell Sci 109:1347–1357. <https://doi.org/10.1242/jcs.109.6.1347>.
- Marguerat S, Schmidt A, Codlin S, Chen W, Aebersold R, Bähler J. 2012. Quantitative analysis of fission yeast transcriptomes and proteomes in proliferating and quiescent cells. Cell 151:671–683. <https://doi.org/10.1016/j.cell.2012.09.019>.
- Gangloff S, Arcangioli B. 2017. DNA repair and mutations during quiescence in yeast. FEMS Yeast Res 17:fox002. <https://doi.org/10.1093/femsyr/fox002>.
- Coluccio AE, Rodriguez RK, Kernan MJ, Neiman AM. 2008. The yeast spore wall enables spores to survive passage through the digestive tract of Drosophila. PLoS One 3:e2873. <https://doi.org/10.1371/journal.pone.0002873>.
- Darwin C. 1871. The descent of man, and selection in relation to sex. John Murray, London, England.
- Beach DH, Klar AJ. 1984. Rearrangements of the transposable mating-type cassettes of fission yeast. EMBO J 3:603–610. <https://doi.org/10.1002/j.1460-2075.1984.tb01855.x>.
- Jeffares DC, Rallis C, Rieux A, Speed D, Převorovský M, Mourier T, Marsellach FX, Iqbal Z, Lau W, Cheng TMK, Pracana R, Müllender M, Lawson JLD, Chessel A, Bala S, Hellenthal G, O'Fallon B, Keane T, Simpson JT, Bischof L, Tomiczek B, Bitton DA, Sideri T, Codlin S, Hellberg JEEU, van Trigt L, Jeffery L, Li J-J, Atkinson S, Thodberg M, Febrer M, McLay K, Drou N, Brown W, Hayles J, Salas REC, Ralsler M, Maniatis N, Balding DJ, Balloux F, Durbin R, Bähler J. 2015. The genomic and phenotypic diversity of Schizosaccharomyces pombe. Nat Genet 47:235–241. <https://doi.org/10.1038/ng.3215>.
- Hu W, Jiang Z-D, Suo F, Zheng J-X, He W-Z, Du L-L. 2017. A large gene family in fission yeast encodes spore killers that subvert Mendel's law. Elife 6:e26057. <https://doi.org/10.7554/eLife.26057>.
- Nuckolls NL, Núñez MAB, Eickbush MT, Young JM, Lange JJ, Yu JS, Smith GR, Jaspersen SL, Malik HS, Zanders SE. 2017. wtf genes are prolific dual poison-antidote meiotic drivers. Elife 6:e26033. <https://doi.org/10.7554/eLife.26033>.
- Tusso S, Nieuwenhuis BPS, Sedlazeck FJ, Davey JW, Jeffares DC, Wolf JBW. 2019. Ancestral admixture is the main determinant of global biodiversity in fission yeast. Mol Biol Evol 36:1975–1989. <https://doi.org/10.1093/molbev/msz126>.
- Hernández JFL, Helston RM, Lange JJ, Billmyre RB, Schaffner SH, Eickbush MT, McCroskey S, Zanders SE. 2021. Diverse mating phenotypes impact the spread of wtf meiotic drivers in Schizosaccharomyces pombe. Elife 10:e70812. <https://doi.org/10.7554/eLife.70812>.
- Wood V, Gwilliam R, Rajandream M-A, Lyne M, Lyne R, Stewart A, Sgouros J, Peat N, Hayles J, Baker S, Basham D, Bowman S, Brooks K, Brown D, Brown S,

- Chillingworth T, Churcher C, Collins M, Connor R, Cronin A, Davis P, Feltwell T, Fraser A, Gentles S, Goble A, Hamlin N, Harris D, Hidalgo J, Hodgson G, Holroyd S, Hornsby T, Howarth S, Huckle EJ, Hunt S, Jagels K, James K, Jones L, Jones M, Leather S, McDonald S, McLean J, Mooney P, Moule S, Mungall K, Murphy L, Niblett D, Odell C, Oliver K, O'Neil S, Pearson D, et al. 2002. The genome sequence of *Schizosaccharomyces pombe*. *Nature* 415:871–880. <https://doi.org/10.1038/nature01203>.
24. Seike T, Sakata N, Matsuda F, Furusawa C. 2021. Elevated sporulation efficiency in fission yeast *Schizosaccharomyces japonicus* strains isolated from *Drosophila*. *J Fungi* 7:350. <https://doi.org/10.3390/jof7050350>.
 25. Brysch-Herzberg M, Jia G-S, Seidel M, Assali I, Du L-L. 2022. Insights into the ecology of *Schizosaccharomyces* species in natural and artificial habitats. *Antonie Van Leeuwenhoek* 115:661–695. <https://doi.org/10.1007/s10482-022-01720-0>.
 26. Fantes P, Nurse P. 1977. Control of cell size at division in fission yeast by a growth-modulated size control over nuclear division. *Exp Cell Res* 107:377–386. [https://doi.org/10.1016/0014-4827\(77\)90359-7](https://doi.org/10.1016/0014-4827(77)90359-7).
 27. Nurse P, Bissett Y. 1981. Gene required in G1 for commitment to cell cycle and in G2 for control of mitosis in fission yeast. *Nature* 292:558–560. <https://doi.org/10.1038/292558a0>.
 28. García-Blanco N, Vázquez-Bolado A, Moreno S. 2019. Greatwall-Endosulfine: a molecular switch that regulates PP2A/B55 protein phosphatase activity in dividing and quiescent cells. *Int J Mol Sci* 20:6228. <https://doi.org/10.3390/ijms20246228>.
 29. Sugimoto A, Iino Y, Maeda T, Watanabe Y, Yamamoto M. 1991. *Schizosaccharomyces pombe* ste11⁺ encodes a transcription factor with an HMG motif that is a critical regulator of sexual development. *Genes Dev* 5:1990–1999. <https://doi.org/10.1101/gad.5.11.1990>.
 30. Mata J, Bähler J. 2006. Global roles of Ste11p, cell type, and pheromone in the control of gene expression during early sexual differentiation in fission yeast. *Proc Natl Acad Sci U S A* 103:15517–15522. <https://doi.org/10.1073/pnas.0603403103>.
 31. Xue-Franzen Y, Kjærulff S, Holmberg C, Wright A, Nielsen O. 2006. Genome-wide identification of pheromone-targeted transcription in fission yeast. *BMC Genomics* 7:303. <https://doi.org/10.1186/1471-2164-7-303>.
 32. Anandhakumar J, Fauquenoy S, Materne P, Migeot V, Hermand D. 2013. Regulation of entry into gametogenesis by Ste11: the endless game. *Biochem Soc Trans* 41:1673–1678. <https://doi.org/10.1042/BST20130225>.
 33. Kelly M, Burke J, Smith M, Klar A, Beach D. 1988. Four mating-type genes control sexual differentiation in the fission yeast. *EMBO J* 7:1537–1547. <https://doi.org/10.1002/j.1460-2075.1988.tb02973.x>.
 34. Sinclair AH, Berta P, Palmer MS, Hawkins JR, Griffiths BL, Smith MJ, Foster JW, Frischauf A-M, Lovell-Badge R, Goodfellow PN. 1990. A gene from the human sex-determining region encodes a protein with homology to a conserved DNA-binding motif. *Nature* 346:240–244. <https://doi.org/10.1038/346240a0>.
 35. Lee J-H, Lin H, Joo S, Goodenough U. 2008. Early sexual origins of homeoprotein heterodimerization and evolution of the plant KNOX/BELL family. *Cell* 133:829–840. <https://doi.org/10.1016/j.cell.2008.04.028>.
 36. Yabana N, Yamamoto M. 1996. *Schizosaccharomyces pombe* map1⁺ encodes a MADS-box-family protein required for cell-type-specific gene expression. *Mol Cell Biol* 16:3420–3428. <https://doi.org/10.1128/MCB.16.7.3420>.
 37. Nielsen O, Friis T, Kjærulff S. 1996. The *Schizosaccharomyces pombe* map1 gene encodes an SRF/MCM1-related protein required for P-cell specific gene expression. *Mol Gen Genet* 253:387–392. <https://doi.org/10.1007/pl00008604>.
 38. Seike T, Nakamura T, Shimoda C. 2013. Distal and proximal actions of peptide pheromone M-factor control different conjugation steps in fission yeast. *PLoS One* 8:e69491. <https://doi.org/10.1371/journal.pone.0069491>.
 39. Sieber B, Coronas-Serna JM, Martin SG. 2022. A focus on yeast mating: from pheromone signaling to cell-cell fusion. *Semin Cell Dev Biol* 133:83–95. <https://doi.org/10.1016/j.semcdb.2022.02.003>.
 40. Harigaya Y, Yamamoto M. 2007. Molecular mechanisms underlying the mitosis-meiosis decision. *Chromosome Res* 15:523–537. <https://doi.org/10.1007/s10577-007-1151-0>.
 41. Vještica A, Bérard M, Liu G, Merlini L, Nkosi PJ, Martin SG. 2021. Cell cycle-dependent and independent mating blocks ensure fungal zygote survival and ploidy maintenance. *PLoS Biol* 19:e3001067. <https://doi.org/10.1371/journal.pbio.3001067>.
 42. Vještica A, Merlini L, Nkosi PJ, Martin SG. 2018. Gamete fusion triggers bipartite transcription factor assembly to block re-fertilization. *Nature* 560:397–400. <https://doi.org/10.1038/s41586-018-0407-5>.
 43. Forsburg SL, Rhind N. 2006. Basic methods for fission yeast. *Yeast* 23:173–183. <https://doi.org/10.1002/yea.1347>.
 44. Shimanuki M, Chung S, Chikashige Y, Kawasaki Y, Uehara L, Tsutsumi C, Hatanaka M, Hiraoka Y, Nagao K, Yanagida M. 2007. Two-step, extensive alterations in the transcriptome from G0 arrest to cell division in *Schizosaccharomyces pombe*. *Genes Cells* 12:677–692. <https://doi.org/10.1111/j.1365-2443.2007.01079.x>.
 45. Takeda K, Yoshida T, Kikuchi S, Nagao K, Kokubu A, Pluskal T, Villar-Briones A, Nakamura T, Yanagida M. 2010. Synergistic roles of the proteasome and autophagy for mitochondrial maintenance and chronological lifespan in fission yeast. *Proc Natl Acad Sci U S A* 107:3540–3545. <https://doi.org/10.1073/pnas.0911055107>.
 46. Mochida S, Yanagida M. 2006. Distinct modes of DNA damage response in *S. pombe* G0 and vegetative cells. *Genes Cells* 11:13–27. <https://doi.org/10.1111/j.1365-2443.2005.00917.x>.
 47. Hassine SB, Arcangioli B. 2009. Tdp1 protects against oxidative DNA damage in non-dividing fission yeast. *EMBO J* 28:632–640. <https://doi.org/10.1038/emboj.2009.9>.
 48. Gangloff S, Achaz G, Francesconi S, Villain A, Miled S, Denis C, Arcangioli B. 2017. Quiescence unveils a novel mutational force in fission yeast. *Elife* 6:e27469. <https://doi.org/10.7554/eLife.27469>.
 49. Egel R, Eie B. 1987. Cell lineage asymmetry in *Schizosaccharomyces pombe*: unilateral transmission of a high-frequency state for mating-type switching in diploid pedigrees. *Curr Genet* 12:429–433. <https://doi.org/10.1007/BF00434820>.
 50. Klar AJS. 1987. Differentiated parental DNA strands confer developmental asymmetry on daughter cells in fission yeast. *Nature* 326:466–470. <https://doi.org/10.1038/326466a0>.
 51. Egel R. 1984. Two tightly linked silent cassettes in the mating-type region of *Schizosaccharomyces pombe*. *Curr Genet* 8:199–203. <https://doi.org/10.1007/BF00417816>.
 52. Thon G, Klar AJ. 1993. Directionality of fission yeast mating-type interconversion is controlled by the location of the donor loci. *Genetics* 134:1045–1054. <https://doi.org/10.1093/genetics/134.4.1045>.
 53. Klar AJ. 1990. The developmental fate of fission yeast cells is determined by the pattern of inheritance of parental and grandparental DNA strands. *EMBO J* 9:1407–1415. <https://doi.org/10.1002/j.1460-2075.1990.tb08256.x>.
 54. Arcangioli B, Klar AJ. 1991. A novel switch-activating site (SAS1) and its cognate binding factor (SAP1) required for efficient mat1 switching in *Schizosaccharomyces pombe*. *EMBO J* 10:3025–3032. <https://doi.org/10.1002/j.1460-2075.1991.tb07853.x>.
 55. Klar AJS, Ishikawa K, Moore S. 2014. A unique DNA recombination mechanism of the mating/cell-type switching of fission yeasts: a review. *Microbiol Spectr* 2:MDNA3-0003-2014. <https://doi.org/10.1128/microbiolspec.MDNA3-0003-2014>.
 56. Jakociūnas T, Holm LR, Verhein-Hansen J, Trusina A, Thon G. 2013. Two portable recombination enhancers direct donor choice in fission yeast heterochromatin. *PLoS Genet* 9:e1003762. <https://doi.org/10.1371/journal.pgen.1003762>.
 57. Maki T, Ogura N, Haber JE, Iwasaki H, Thon G. 2018. New insights into donor directionality of mating-type switching in *Schizosaccharomyces pombe*. *PLoS Genet* 14:e1007424. <https://doi.org/10.1371/journal.pgen.1007424>.
 58. Zion EH, Chandrasekhara C, Chen X. 2020. Asymmetric inheritance of epigenetic states in asymmetrically dividing stem cells. *Curr Opin Cell Biol* 67:27–36. <https://doi.org/10.1016/j.cob.2020.08.003>.
 59. Ranjan R, Chen X. 2022. Mitotic drive in asymmetric epigenetic inheritance. *Biochem Soc Trans* 50:675–688. <https://doi.org/10.1042/BST20200267>.
 60. Klar AJS. 2007. Lessons learned from studies of fission yeast mating-type switching and silencing. *Annu Rev Genet* 41:213–236. <https://doi.org/10.1146/annurev.genet.39.073103.094316>.
 61. Beach D, Nurse P, Egel R. 1982. Molecular rearrangement of mating-type genes in fission yeast. *Nature* 296:682–683. <https://doi.org/10.1038/296682a0>.
 62. Beach DH. 1983. Cell type switching by DNA transposition in fission yeast. *Nature* 305:682–688. <https://doi.org/10.1038/305682a0>.
 63. Grewal SIS, Klar AJS. 1996. Chromosomal inheritance of epigenetic states in fission yeast during mitosis and meiosis. *Cell* 86:95–101. [https://doi.org/10.1016/S0092-8674\(00\)80080-X](https://doi.org/10.1016/S0092-8674(00)80080-X).
 64. Thon G, Friis T. 1997. Epigenetic inheritance of transcriptional silencing and switching competence in fission yeast. *Genetics* 145:685–696. <https://doi.org/10.1093/genetics/145.3.685>.
 65. Klar AJ, Bonaduce MJ, Cafferkey R. 1991. The mechanism of fission yeast mating type interconversion: seal/replicate/cleave model of replication across the double-stranded break site at mat1. *Genetics* 127:489–496. <https://doi.org/10.1093/genetics/127.3.489>.
 66. Grewal SIS, Klar AJS. 1997. A recombinationally repressed region between mat2 and mat3 loci shares homology to centromeric repeats and regulates

- directionality of mating-type switching in fission yeast. *Genetics* 146:1221–1238. <https://doi.org/10.1093/genetics/146.4.1221>.
67. Thon G, Bjering KP, Nielsen IS. 1999. Localization and properties of a silencing element near the mat3-M mating-type cassette of *Schizosaccharomyces pombe*. *Genetics* 151:945–963. <https://doi.org/10.1093/genetics/151.3.945>.
 68. Ayoub N, Goldshmidt I, Lyakhovetsky R, Cohen A. 2000. A fission yeast repression element cooperates with centromere-like sequences and defines a mat silent domain boundary. *Genetics* 156:983–994. <https://doi.org/10.1093/genetics/156.3.983>.
 69. Ayoub N, Goldshmidt I, Cohen A. 1999. Position effect variegation at the mating-type locus of fission yeast: a cis-acting element inhibits covariegated expression of genes in the silent and expressed domains. *Genetics* 152:495–508. <https://doi.org/10.1093/genetics/152.2.495>.
 70. Hansen KR, Hazan I, Shanker S, Watt S, Verhein-Hansen J, Bähler J, Martienssen RA, Partridge JF, Cohen A, Thon G. 2011. H3K9me-independent gene silencing in fission yeast heterochromatin by Clr5 and histone deacetylases. *PLoS Genet* 7:e1001268. <https://doi.org/10.1371/journal.pgen.1001268>.
 71. Noma K, Cam HP, Maraja RJ, Grewal SIS. 2006. A role for TFIIIC transcription factor complex in genome organization. *Cell* 125:859–872. <https://doi.org/10.1016/j.cell.2006.04.028>.
 72. Charlton SJ, Jørgensen MM, Thon G. 2020. Integrity of a heterochromatic domain ensured by its boundary elements. *Proc Natl Acad Sci U S A* 117:21504–21511. <https://doi.org/10.1073/pnas.2010062117>.
 73. Wang X, Paulo JA, Li X, Zhou H, Yu J, Gygi SP, Moazed D. 2021. A composite DNA element that functions as a maintainer required for epigenetic inheritance of heterochromatin. *Mol Cell* 81:3979–3991.e4. <https://doi.org/10.1016/j.molcel.2021.07.017>.
 74. Nielsen O, Egel R. 1989. Mapping the double-strand breaks at the mating-type locus in fission yeast by genomic sequencing. *EMBO J* 8:269–276. <https://doi.org/10.1002/j.1460-2075.1989.tb03373.x>.
 75. Gutz H, Schmidt H. 1985. Switching genes in *Schizosaccharomyces pombe*. *Curr Genet* 9:325–331. <https://doi.org/10.1007/BF00421601>.
 76. Strathern JN, Klar AJS, Hicks JB, Abraham JA, Ivy JM, Nasmyth KA, McGill C. 1982. Homothallic switching of yeast mating type cassettes is initiated by a double-stranded cut in the MAT locus. *Cell* 31:183–192. [https://doi.org/10.1016/0092-8674\(82\)90418-4](https://doi.org/10.1016/0092-8674(82)90418-4).
 77. Szostak JW, Orr-Weaver TL, Rothstein RJ, Stahl FW. 1983. The double-strand-break repair model for recombination. *Cell* 33:25–35. [https://doi.org/10.1016/0092-8674\(83\)90331-8](https://doi.org/10.1016/0092-8674(83)90331-8).
 78. Cosma MP. 2004. Daughter-specific repression of *Saccharomyces cerevisiae* HO: Ash1 is the commander. *EMBO Rep* 5:953–957. <https://doi.org/10.1038/sj.embor.7400251>.
 79. Klar AJS, Miglio LM. 1986. Initiation of meiotic recombination by double-strand DNA breaks in *S. pombe*. *Cell* 46:725–731. [https://doi.org/10.1016/0092-8674\(86\)90348-x](https://doi.org/10.1016/0092-8674(86)90348-x).
 80. Roseaulin L, Yamada Y, Tsutsui Y, Russell P, Iwasaki H, Arcangioli B. 2008. Mus81 is essential for sister chromatid recombination at broken replication forks. *EMBO J* 27:1378–1387. <https://doi.org/10.1038/emboj.2008.65>.
 81. Klar AJS, Strathern JN, Abraham JA. 1984. Involvement of double-strand chromosomal breaks for mating-type switching in *Saccharomyces cerevisiae*. *Cold Spring Harbor Symp Quant Biol* 49:77–88. <https://doi.org/10.1101/sqb.1984.049.01.011>.
 82. Arcangioli B. 1998. A site- and strand-specific DNA break confers asymmetric switching potential in fission yeast. *EMBO J* 17:4503–4510. <https://doi.org/10.1093/emboj/17.15.4503>.
 83. Dalgaard JZ, Klar AJS. 1999. Orientation of DNA replication establishes mating-type switching pattern in *S. pombe*. *Nature* 400:181–184. <https://doi.org/10.1038/22139>.
 84. Vengrova S, Dalgaard JZ. 2004. RNase-sensitive DNA modification(s) initiates *S. pombe* mating-type switching. *Genes Dev* 18:794–804. <https://doi.org/10.1101/gad.289404>.
 85. Vengrova S, Dalgaard JZ. 2006. The wild-type *Schizosaccharomyces pombe* mat1 imprint consists of two ribonucleotides. *EMBO Rep* 7:59–65. <https://doi.org/10.1038/sj.embor.7400576>.
 86. Kaykov A, Arcangioli B. 2004. A programmed strand-specific and modified nick in *S. pombe* constitutes a novel type of chromosomal imprint. *Curr Biol* 14:1924–1928. <https://doi.org/10.1016/j.cub.2004.10.026>.
 87. Sayrac S, Vengrova S, Godfrey EL, Dalgaard JZ. 2011. Identification of a novel type of spacer element required for imprinting in fission yeast. *PLoS Genet* 7:e1001328. <https://doi.org/10.1371/journal.pgen.1001328>.
 88. Raimondi C, Jagla B, Proux C, Waxin H, Gangloff S, Arcangioli B. 2018. Molecular signature of the imprintosome complex at the mating-type locus in fission yeast. *Microb Cell* 5:169–183. <https://doi.org/10.15698/mic2018.04.623>.
 89. Cao B, Wu X, Zhou J, Wu H, Liu L, Zhang Q, DeMott MS, Gu C, Wang L, You D, Dedon PC. 2020. Nick-seq for single-nucleotide resolution genomic maps of DNA modifications and damage. *Nucleic Acids Res* 48:6715–6725. <https://doi.org/10.1093/nar/gkaa473>.
 90. Cao H, Salazar-García L, Gao F, Wahlestedt T, Wu C-L, Han X, Cai Y, Xu D, Wang F, Tang L, Ricciardi N, Cai D, Wang H, Chin MPS, Timmons JA, Wahlestedt C, Kapranov P. 2019. Novel approach reveals genomic landscapes of single-strand DNA breaks with nucleotide resolution in human cells. *Nat Commun* 10:5799. <https://doi.org/10.1038/s41467-019-13602-7>.
 91. Sriramachandran AM, Petrosino G, Méndez-Lago M, Schäfer AJ, Batista-Nascimento LS, Zilio N, Ulrich HD. 2020. Genome-wide nucleotide-resolution mapping of DNA replication patterns, single-strand breaks, and lesions by GLOE-Seq. *Mol Cell* 78:975–985.e7. <https://doi.org/10.1016/j.molcel.2020.03.027>.
 92. Maundrell K, Hutchison A, Shall S. 1988. Sequence analysis of ARS elements in fission yeast. *EMBO J* 7:2203–2209. <https://doi.org/10.1002/j.1460-2075.1988.tb03059.x>.
 93. Dalgaard JZ, Klar AJS. 2000. swi1 and swi3 perform imprinting, pausing, and termination of DNA replication in *S. pombe*. *Cell* 102:745–751. [https://doi.org/10.1016/S0092-8674\(00\)00063-5](https://doi.org/10.1016/S0092-8674(00)00063-5).
 94. Dalgaard JZ, Klar AJS. 2001. Does *S. pombe* exploit the intrinsic asymmetry of DNA synthesis to imprint daughter cells for mating-type switching? *Trends Genet* 17:153–157. [https://doi.org/10.1016/S0168-9525\(00\)02203-4](https://doi.org/10.1016/S0168-9525(00)02203-4).
 95. Codlin S, Dalgaard JZ. 2003. Complex mechanism of site-specific DNA replication termination in fission yeast. *EMBO J* 22:3431–3440. <https://doi.org/10.1093/emboj/cdg330>.
 96. Egel R, Willer M, Kjaerulff S, Davey J, Nielsen O. 1994. Assessment of pheromone production and response in fission yeast by a halo test of induced sporulation. *Yeast* 10:1347–1354. <https://doi.org/10.1002/yea.320101012>.
 97. Noguchi C, Noguchi E. 2007. Sap1 promotes the association of the replication fork protection complex with chromatin and is involved in the replication checkpoint in *Schizosaccharomyces pombe*. *Genetics* 175:553–566. <https://doi.org/10.1534/genetics.106.065334>.
 98. Baris Y, Taylor MRG, Aria V, Yeeles JTP. 2022. Fast and efficient DNA replication with purified human proteins. *Nature* 606:204–210. <https://doi.org/10.1038/s41586-022-04759-1>.
 99. Zech J, Godfrey EL, Masai H, Hartsuiker E, Dalgaard JZ. 2015. The DNA-binding domain of *S. pombe* Mrc1 (Claspin) acts to enhance stalling at replication barriers. *PLoS One* 10:e0132595. <https://doi.org/10.1371/journal.pone.0132595>.
 100. Singh J, Klar AJS. 1993. DNA polymerase- α is essential for mating-type switching in fission yeast. *Nature* 361:271–273. <https://doi.org/10.1038/361271a0>.
 101. Singh B, Bisht KK, Upadhyay U, Kushwaha AC, Nanda JS, Srivastava S, Saini JK, Klar AJS, Singh J. 2019. Role of Cdc23/Mcm10 in generating the ribonucleotide imprint at the mat1 locus in fission yeast. *Nucleic Acids Res* 47:3422–3433. <https://doi.org/10.1093/nar/gkz092>.
 102. Fien K, Hurwitz J. 2006. Fission yeast Mcm10p contains primase activity. *J Biol Chem* 281:22248–22260. <https://doi.org/10.1074/jbc.M512997200>.
 103. Baxley R, Bielinsky A-K. 2017. Mcm10: a dynamic scaffold at eukaryotic replication forks. *Genes (Basel)* 8:73. <https://doi.org/10.3390/genes8020073>.
 104. Thu YM, Bielinsky A-K. 2013. Enigmatic roles of Mcm10 in DNA replication. *Trends Biochem Sci* 38:184–194. <https://doi.org/10.1016/j.tibs.2012.12.003>.
 105. Kang Z, Fu P, Alcivar AL, Fu H, Redon C, Foo TK, Zuo Y, Ye C, Baxley R, Madireddy A, Buisson R, Bielinsky A-K, Zou L, Shen Z, Aladjem MI, Xia B. 2021. BRCA2 associates with MCM10 to suppress PRIMPOL-mediated repriming and single-stranded gap formation after DNA damage. *Nat Commun* 12:5966. <https://doi.org/10.1038/s41467-021-26227-6>.
 106. Holmes AM, Kaykov A, Arcangioli B. 2005. Molecular and cellular dissection of mating-type switching steps in *Schizosaccharomyces pombe*. *Mol Cell Biol* 25:303–311. <https://doi.org/10.1128/MCB.25.1.303-311.2005>.
 107. Styrkársdóttir U, Egel R, Nielsen O. 1993. The smt-0 mutation which abolishes mating-type switching in fission yeast is a deletion. *Curr Genet* 23:184–186. <https://doi.org/10.1007/BF00352020>.
 108. Kaykov A, Holmes AM, Arcangioli B. 2004. Formation, maintenance and consequences of the imprint at the mating-type locus in fission yeast. *EMBO J* 23:930–938. <https://doi.org/10.1038/sj.emboj.7600099>.
 109. Singh J. 2019. RNA insertion in DNA as the imprint moiety: the fission yeast paradigm. *Curr Genet* 65:1301–1306. <https://doi.org/10.1007/s00294-019-00991-x>.
 110. Kim S-M, Dubey DD, Huberman JA. 2003. Early-replicating heterochromatin. *Genes Dev* 17:330–335. <https://doi.org/10.1101/gad.1046203>.

111. Holmes A, Roseaulin L, Schurra C, Waxin H, Lambert S, Zaratiegui M, Martienssen RA, Arcangioli B. 2012. Lsd1 and Lsd2 control programmed replication fork pauses and imprinting in fission yeast. *Cell Rep* 2: 1513–1520. <https://doi.org/10.1016/j.celrep.2012.10.011>.
112. Chosed R, Dent SYR. 2007. A two-way street: LSD1 regulates chromatin boundary formation in *S. pombe* and *Drosophila*. *Mol Cell* 26:160–162. <https://doi.org/10.1016/j.molcel.2007.04.009>.
113. Lan F, Zaratiegui M, Villén J, Vaughn MW, Verdel A, Huarte M, Shi Y, Gygi SP, Moazed D, Martienssen RA, Shi Y. 2007. *S. pombe* LSD1 homologs regulate heterochromatin propagation and euchromatic gene transcription. *Mol Cell* 26:89–101. <https://doi.org/10.1016/j.molcel.2007.02.023>.
114. Gordon M, Holt DG, Panigrahi A, Wilhelm BT, Erdjument-Bromage H, Tempst P, Bähler J, Cairns BR. 2007. Genome-wide dynamics of SAPHIRE, an essential complex for gene activation and chromatin boundaries. *Mol Cell Biol* 27:4058–4069. <https://doi.org/10.1128/MCB.02044-06>.
115. Nicolas E, Lee MG, Hakimi M-A, Cam HP, Grewal SIS, Shiekhatter R. 2006. Fission yeast homologs of human histone H3 lysine 4 demethylase regulate a common set of genes with diverse functions. *J Biol Chem* 281: 35983–35988. <https://doi.org/10.1074/jbc.M606349200>.
116. Lan F, Collins RE, Cegli RD, Alpatov R, Horton JR, Shi X, Gozani O, Cheng X, Shi Y. 2007. Recognition of unmethylated histone H3 lysine 4 links BHC80 to LSD1-mediated gene repression. *Nature* 448:718–722. <https://doi.org/10.1038/nature06034>.
117. Marmorstein LY, Kinev AV, Chan GKT, Bochar DA, Beniya H, Epstein JA, Yen TJ, Shiekhatter R. 2001. A human BRCA2 complex containing a structural DNA binding component influences cell cycle progression. *Cell* 104:247–257. [https://doi.org/10.1016/S0092-8674\(01\)00209-4](https://doi.org/10.1016/S0092-8674(01)00209-4).
118. Wang Y, Huang Y, Cheng E, Liu X, Zhang Y, Yang J, Young JTF, Brown GW, Yang X, Shang Y. 2022. LSD1 is required for euchromatic origin firing and replication timing. *Signal Transduct Target Ther* 7:102. <https://doi.org/10.1038/s41392-022-00927-x>.
119. Li F, Huarte M, Zaratiegui M, Vaughn MW, Shi Y, Martienssen R, Cande WZ. 2008. Lid2 is required for coordinating H3K4 and H3K9 methylation of heterochromatin and euchromatin. *Cell* 135:272–283. <https://doi.org/10.1016/j.cell.2008.08.036>.
120. Marayati BF, Tucker JF, Cerda DADL, Hou T-C, Chen R, Sugiyama T, Pease JB, Zhang K. 2020. The catalytic-dependent and -independent roles of Lsd1 and Lsd2 lysine demethylases in heterochromatin formation in *Schizosaccharomyces pombe*. *Cells* 9:955. <https://doi.org/10.3390/cells9040955>.
121. Mejía-Ramírez E, Sánchez-Gorostiaga A, Krimer DB, Schwartzman JB, Hernández P. 2005. The mating type switch-activating protein Sap1 is required for replication fork arrest at the rRNA genes of fission yeast. *Mol Cell Biol* 25: 8755–8761. <https://doi.org/10.1128/MCB.25.19.8755-8761.2005>.
122. Zaratiegui M, Vaughn MW, Irvine DV, Goto D, Watt S, Bähler J, Arcangioli B, Martienssen RA. 2011. CENP-B preserves genome integrity at replication forks paused by retrotransposon LTR. *Nature* 469:112–115. <https://doi.org/10.1038/nature09608>.
123. Arcangioli B. 1992. A switch in time. *Curr Biol* 2:323–325. [https://doi.org/10.1016/0960-9822\(92\)90895-h](https://doi.org/10.1016/0960-9822(92)90895-h).
124. Klar AJ, Bonaduce MJ. 1993. The mechanism of fission yeast mating-type interconversion: evidence for two types of epigenetically inherited chromosomal imprinted events. *Cold Spring Harbor Symp Quant Biol* 58: 457–465. <https://doi.org/10.1101/sqb.1993.058.01.052>.
125. Shyian M, Shore D. 2021. Approaching protein barriers: emerging mechanisms of replication pausing in eukaryotes. *Frontiers Cell Dev Biol* 9: 672510. <https://doi.org/10.3389/fcell.2021.672510>.
126. Sánchez-Gorostiaga A, López-Estraño C, Krimer DB, Schwartzman JB, Hernández P. 2004. Transcription termination factor reb1p causes two replication fork barriers at its cognate sites in fission yeast ribosomal DNA in vivo. *Mol Cell Biol* 24:398–406. <https://doi.org/10.1128/MCB.24.1.398-406.2004>.
127. Krings G, Bastia D. 2006. Molecular architecture of a eukaryotic DNA replication terminus-terminator protein complex. *Mol Cell Biol* 26:8061–8074. <https://doi.org/10.1128/MCB.01102-06>.
128. Win TZ, Mankouri HW, Hickson ID, Wang S-W. 2005. A role for the fission yeast Rqh1 helicase in chromosome segregation. *J Cell Sci* 118:5777–5784. <https://doi.org/10.1242/jcs.02694>.
129. Jalan M, Oehler J, Morrow CA, Osman F, Whitby MC. 2019. Factors affecting template switch recombination associated with restarted DNA replication. *Elife* 8:e41697. <https://doi.org/10.7554/eLife.41697>.
130. Tamang S, Kishkevich A, Morrow CA, Osman F, Jalan M, Whitby MC. 2019. The PCNA unloader Elg1 promotes recombination at collapsed replication forks in fission yeast. *Elife* 8:e47277. <https://doi.org/10.7554/eLife.47277>.
131. Lambert S, Watson A, Sheedy DM, Martin B, Carr AM. 2005. Gross chromosomal rearrangements and elevated recombination at an inducible site-specific replication fork barrier. *Cell* 121:689–702. <https://doi.org/10.1016/j.cell.2005.03.022>.
132. Ahn JS, Osman F, Whitby MC. 2005. Replication fork blockage by RTS1 at an ectopic site promotes recombination in fission yeast. *EMBO J* 24: 2011–2023. <https://doi.org/10.1038/sj.emboj.7600670>.
133. Mizuno K, Lambert S, Baldacci G, Murray JM, Carr AM. 2009. Nearby inverted repeats fuse to generate acentric and dicentric palindromic chromosomes by a replication template exchange mechanism. *Genes Dev* 23:2876–2886. <https://doi.org/10.1101/gad.1863009>.
134. Saada AA, Lambert SAE, Carr AM. 2018. Preserving replication fork integrity and competence via the homologous recombination pathway. *DNA Repair (Amst)* 71:135–147. <https://doi.org/10.1016/j.dnarep.2018.08.017>.
135. Kramara J, Osia B, Malkova A. 2018. Break-induced replication: the where, the why, and the how. *Trends Genet* 34:518–531. <https://doi.org/10.1016/j.tig.2018.04.002>.
136. Carr A, Lambert S. 2021. Recombination-dependent replication: new perspectives from site-specific fork barriers. *Curr Opin Genet Dev* 71: 129–135. <https://doi.org/10.1016/j.gde.2021.07.008>.
137. Marie L, Symington LS. 2022. Mechanism for inverted-repeat recombination induced by a replication fork barrier. *Nat Commun* 13:32. <https://doi.org/10.1038/s41467-021-27443-w>.
138. Mayle R, Campbell IM, Beck CR, Yu Y, Wilson M, Shaw CA, Bjergbaek L, Lupski JR, Ira G. 2015. Mus81 and converging forks limit the mutagenicity of replication fork breakage. *Science* 349:742–747. <https://doi.org/10.1126/science.aaa8391>.
139. Donnianni RA, Symington LS. 2013. Break-induced replication occurs by conservative DNA synthesis. *Proc Natl Acad Sci U S A* 110:13475–13480. <https://doi.org/10.1073/pnas.1309800110>.
140. Naiman K, Campillo-Funollet E, Watson AT, Budden A, Miyabe I, Carr AM. 2021. Replication dynamics of recombination-dependent replication forks. *Nat Commun* 12:923. <https://doi.org/10.1038/s41467-021-21198-0>.
141. Tye S, Ronson GE, Morris JR. 2021. A fork in the road: where homologous recombination and stalled replication fork protection part ways. *Semin Cell Dev Biol* 113:14–26. <https://doi.org/10.1016/j.semcdb.2020.07.004>.
142. Epum EA, Haber JE. 2022. DNA replication: the recombination connection. *Trends Cell Biol* 32:45–57. <https://doi.org/10.1016/j.tcb.2021.07.005>.
143. Arcangioli B, de Lahondès R. 2000. Fission yeast switches mating type by a replication–recombination coupled process. *EMBO J* 19:1389–1396. <https://doi.org/10.1093/emboj/19.6.1389>.
144. Fleck O, Rudolph C, Albrecht A, Lorentz A, Schär P, Schmidt H. 1994. The mutator gene swi8 effects specific mutations in the mating-type region of *Schizosaccharomyces pombe*. *Genetics* 138:621–632. <https://doi.org/10.1093/genetics/138.3.621>.
145. Liu L, Yan Z, Osia BA, Twarowski J, Sun L, Kramara J, Lee R, Kumar S, Elango R, Li H, Dang W, Ira G, Malkova A. 2021. Tracking break induced replication reveals its stalling at roadblocks. *Nature* 590:655–659. <https://doi.org/10.1038/s41586-020-03172-w>.
146. Schmidt H, Kapitzka-Fecke P, Stephen ER, Gutz H. 1989. Some of the swi genes of *Schizosaccharomyces pombe* also have a function in the repair of radiation damage. *Curr Genet* 16:89–94. <https://doi.org/10.1007/BF00393400>.
147. Fleck O, Michael H, Heim L. 1992. The swi4⁺ gene of *Schizosaccharomyces pombe* encodes a homologue of mismatch repair enzymes. *Nucleic Acids Res* 20:2271–2278. <https://doi.org/10.1093/nar/20.9.2271>.
148. Ostermann K, Lorentz A, Schmidt H. 1993. The fission yeast rad22 gene, having a function in mating-type switching and repair of DNA damages, encodes a protein homolog to Rad52 of *Saccharomyces cerevisiae*. *Nucleic Acids Res* 21:5940–5944. <https://doi.org/10.1093/nar/21.25.5940>.
149. Rudolph C, Kunz C, Parisi S, Lehmann E, Hartsuiker E, Fartmann B, Kramer W, Kohli J, Fleck O. 1999. The msh2 gene of *Schizosaccharomyces pombe* is involved in mismatch repair, mating-type switching, and meiotic chromosome organization. *Mol Cell Biol* 19:241–250. <https://doi.org/10.1128/MCB.19.1.241>.
150. Zhang J-M, Liu X-M, Ding Y-H, Xiong L-Y, Ren J-Y, Zhou Z-X, Wang H-T, Zhang M-J, Yu Y, Dong M-Q, Du L-L. 2014. Fission yeast Pxd1 promotes proper DNA repair by activating Rad16XPF and inhibiting Dna2. *PLoS Biol* 12:e1001946. <https://doi.org/10.1371/journal.pbio.1001946>.
151. McGill CB, Shafer BK, Derr LK, Strathern JN. 1993. Recombination initiated by double-strand breaks. *Curr Genet* 23:305–314. <https://doi.org/10.1007/BF00310891>.
152. Haber JE. 1998. Mating-type gene switching in *Saccharomyces cerevisiae*. *Annu Rev Genet* 32:561–599. <https://doi.org/10.1146/annurev.genet.32.1.561>.

153. Lydeard JR, Jain S, Yamaguchi M, Haber JE. 2007. Break-induced replication and telomerase-independent telomere maintenance require Pol32. *Nature* 448:820–823. <https://doi.org/10.1038/nature06047>.
154. Donnianni RA, Zhou Z-X, Lujan SA, Al-Zain A, Garcia V, Glancy E, Burkholder AB, Kunkel TA, Symington LS. 2019. DNA polymerase delta synthesizes both strands during break-induced replication. *Mol Cell* 76:371–381.e4. <https://doi.org/10.1016/j.molcel.2019.07.033>.
155. Arcangioli B. 2000. Fate of mat1 DNA strands during mating-type switching in fission yeast. *EMBO Rep* 1:145–150. <https://doi.org/10.1093/embo-reports/kvd023>.
156. Hyjek M, Figiel M, Nowotny M. 2019. RNases H: structure and mechanism. *DNA Repair (Amst)* 84:102672. <https://doi.org/10.1016/j.dnarep.2019.102672>.
157. Kim N, Huang SN, Williams JS, Li YC, Clark AB, Cho J-E, Kunkel TA, Pommier Y, Jinks-Robertson S. 2011. Mutagenic processing of ribonucleotides in DNA by yeast topoisomerase I. *Science* 332:1561–1564. <https://doi.org/10.1126/science.1205016>.
158. Reijns MAM, Parry DA, Williams TC, Nadeu F, Hindshaw RL, Szwed DOR, Nicholson MD, Carroll P, Boyle S, Royo R, Cornish AJ, Xiang H, Ridout K, Ambrose JC, Arumugam P, Bevers R, Bleda M, Boardman-Pretty F, Bousted CR, Brittain H, Caulfield MJ, Chan GC, Elgar G, Fowler T, Giess A, Hamblin A, Henderson S, Hubbard TJP, Jackson R, Jones LJ, Kasperaviciute D, Kayikci M, Kousathanas A, Lahnstein L, Leigh SEA, Leong IUS, Lopez JF, Maleady-Crowe F, McEntagart M, Minnici F, Moutsianis L, Mueller M, Murugaesu N, Need AC, O'Donovan P, Odhams CA, Patch C, Pereira MB, Perez-Gil D, Pullinger J, Genomics England Research Consortium, Colorectal Cancer Domain UK 100,000 Genomes Project, et al. 2022. Signatures of TOP1 transcription-associated mutagenesis in cancer and germline. *Nature* 602:623–631. <https://doi.org/10.1038/s41586-022-04403-y>.
159. Zhao H, Zhu M, Limbo O, Russell P. 2018. RNase H eliminates R-loops that disrupt DNA replication but is nonessential for efficient DSB repair. *EMBO Rep* 19:e45335. <https://doi.org/10.15252/embr.201745335>.
160. Koulintchenko M, Vengrova S, Eydmann T, Arumugam P, Dalgaard JZ. 2012. DNA polymerase α (swi7) and the flap endonuclease Fen1 (rad2) act together in the S-phase alkylation damage response in *S. pombe*. *PLoS One* 7:e47091. <https://doi.org/10.1371/journal.pone.0047091>.
161. Yamada-Inagawa T, Klar AJS, Dalgaard JZ. 2007. Schizosaccharomyces pombe switches mating type by the synthesis-dependent strand-annealing mechanism. *Genetics* 177:255–265. <https://doi.org/10.1534/genetics.107.076315>.
162. Volpe TA, Kidner C, Hall IM, Teng G, Grewal SIS, Martienssen RA. 2002. Regulation of heterochromatic silencing and histone H3 lysine-9 methylation by RNAi. *Science* 297:1833–1837. <https://doi.org/10.1126/science.1074973>.
163. Provost P, Silverstein RA, Dishart D, Walfridsson J, Djupeal J, Kniola B, Wright A, Samuelsson B, Rådmark O, Ekwall K. 2002. Dicer is required for chromosome segregation and gene silencing in fission yeast cells. *Proc Natl Acad Sci U S A* 99:16648–16653. <https://doi.org/10.1073/pnas.212633199>.
164. Hall IM, Shankaranarayana GD, Noma K, Ayoub N, Cohen A, Grewal SIS. 2002. Establishment and maintenance of a heterochromatin domain. *Science* 297:2232–2237. <https://doi.org/10.1126/science.1076466>.
165. Verdel A, Jia S, Gerber S, Sugiyama T, Gygi S, Grewal SIS, Moazed D. 2004. RNAi-mediated targeting of heterochromatin by the RITS complex. *Science* 303:672–676. <https://doi.org/10.1126/science.1093686>.
166. Lorentz A, Heim L, Schmidt H. 1992. The switching gene swi6 affects recombination and gene expression in the mating-type region of *Schizosaccharomyces pombe*. *Mol Gen Genet* 233:436–442. <https://doi.org/10.1007/BF00265441>.
167. Thon G, Cohen A, Klar AJ. 1994. Three additional linkage groups that repress transcription and meiotic recombination in the mating-type region of *Schizosaccharomyces pombe*. *Genetics* 138:29–38. <https://doi.org/10.1093/genetics/138.1.29>.
168. Ekwall K, Javerzat J-P, Lorentz A, Schmidt H, Cranston G, Allshire R. 1995. The chromodomain protein Swi6: a key component at fission yeast centromeres. *Science* 269:1429–1431. <https://doi.org/10.1126/science.7660126>.
169. Grewal SIS, Bonaduce MJ, Klar AJS. 1998. Histone deacetylase homologs regulate epigenetic inheritance of transcriptional silencing and chromosome segregation in fission yeast. *Genetics* 150:563–576. <https://doi.org/10.1093/genetics/150.2.563>.
170. Nakayama J, Rice JC, Strahl BD, Allis CD, Grewal SIS. 2001. Role of histone H3 lysine 9 methylation in epigenetic control of heterochromatin assembly. *Science* 292:110–113. <https://doi.org/10.1126/science.1060118>.
171. Thon G, Klar AJ. 1992. The clr1 locus regulates the expression of the cryptic mating-type loci of fission yeast. *Genetics* 131:287–296. <https://doi.org/10.1093/genetics/131.2.287>.
172. Ekwall K, Ruusala T. 1994. Mutations in rik1, clr2, clr3 and clr4 genes asymmetrically derepress the silent mating-type loci in fission yeast. *Genetics* 136:53–64. <https://doi.org/10.1093/genetics/136.1.53>.
173. Toda T, Shimanuki M, Yanagida M. 1991. Fission yeast genes that confer resistance to staurosporine encode an AP-1-like transcription factor and a protein kinase related to the mammalian ERK1/MAP2 and budding yeast FUS3 and KSS1 kinases. *Genes Dev* 5:60–73. <https://doi.org/10.1101/gad.5.1.60>.
174. Kumar A, Nanda JS, Saini S, Singh J. 2021. An RNAi-independent role of AP1-like stress response factor Pap1 in centromere and mating-type silencing in *Schizosaccharomyces pombe*. *J Biosci* 46:74. <https://doi.org/10.1007/s12038-021-00199-7>.
175. Obersriebnig MJ, Pallesen EMH, Sneppen K, Trusina A, Thon G. 2016. Nucleation and spreading of a heterochromatic domain in fission yeast. *Nat Commun* 7:11518. <https://doi.org/10.1038/ncomms11518>.
176. Shankaranarayana GD, Motamedi MR, Moazed D, Grewal SIS. 2003. Sir2 regulates histone H3 lysine 9 methylation and heterochromatin assembly in fission yeast. *Curr Biol* 13:1240–1246. [https://doi.org/10.1016/s0960-9822\(03\)00489-5](https://doi.org/10.1016/s0960-9822(03)00489-5).
177. DiPiazza ARC, Taneja N, Dhakshnamoorthy J, Wheeler D, Holla S, Grewal SIS. 2021. Spreading and epigenetic inheritance of heterochromatin require a critical density of histone H3 lysine 9 tri-methylation. *Proc National Acad Sci* 118:e2100699118. <https://doi.org/10.1073/pnas.2100699118>.
178. Jia S, Noma K, Grewal SIS. 2004. RNAi-independent heterochromatin nucleation by the stress-activated ATF/CREB family proteins. *Science* 304:1971–1976. <https://doi.org/10.1126/science.1099035>.
179. Kim HS, Choi ES, Shin JA, Jang YK, Park SD. 2004. Regulation of Swi6/HP1-dependent heterochromatin assembly by cooperation of components of the mitogen-activated protein kinase pathway and a histone deacetylase Clr6. *J Biol Chem* 279:42850–42859. <https://doi.org/10.1074/jbc.M407259200>.
180. Torres-Garcia S, Yaseen I, Shukla M, Audergon PNCB, White SA, Pidoux AL, Allshire RC. 2020. Epigenetic gene silencing by heterochromatin primes fungal resistance. *Nature* 585:453–458. <https://doi.org/10.1038/s41586-020-2706-x>.
181. Hong E-JE, Villén J, Gerace EL, Gygi SP, Moazed D. 2005. A cullin E3 ubiquitin ligase complex associates with Rik1 and the Clr4 histone H3-K9 methyltransferase and is required for RNAi-mediated heterochromatin formation. *RNA Biol* 2:106–111. <https://doi.org/10.4161/rna.2.3.2131>.
182. Li F, Martienssen R, Cande WZ. 2011. Coordination of DNA replication and histone modification by the Rik1–Dos2 complex. *Nature* 475:244–248. <https://doi.org/10.1038/nature10161>.
183. Wang J, Tadeo X, Hou H, Tu PG, Thompson J, Yates JR, Jia S. 2013. Epe1 recruits BET family bromodomain protein Bdf2 to establish heterochromatin boundaries. *Genes Dev* 27:1886–1902. <https://doi.org/10.1101/gad.221010.113>.
184. Ekwall K, Nimmo ER, Javerzat JP, Borgstrom B, Egel R, Cranston G, Allshire R. 1996. Mutations in the fission yeast silencing factors clr4⁺ and rik1⁺ disrupt the localisation of the chromo domain protein Swi6p and impair centromere function. *J Cell Sci* 109:2637–2648. <https://doi.org/10.1242/jcs.109.11.2637>.
185. Ayoub N, Noma K, Isaac S, Kahan T, Grewal SIS, Cohen A. 2003. A novel jmjC domain protein modulates heterochromatinization in fission yeast. *Mol Cell Biol* 23:4356–4370. <https://doi.org/10.1128/MCB.23.12.4356-4370.2003>.
186. Strålfors A, Walfridsson J, Bhuiyan H, Ekwall K. 2011. The FUN30 chromatin remodeler, Fft3, protects centromeric and subtelomeric domains from euchromatin formation. *PLoS Genet* 7:e1001334. <https://doi.org/10.1371/journal.pgen.1001334>.
187. Holla S, Dhakshnamoorthy J, Folco HD, Balachandran V, Xiao H, Sun L, Wheeler D, Zofall M, Grewal SIS. 2020. Positioning heterochromatin at the nuclear periphery suppresses histone turnover to promote epigenetic inheritance. *Cell* 180:150–164.e15. <https://doi.org/10.1016/j.cell.2019.12.004>.
188. Arcangioli B, Copeland TD, Klar AJ. 1994. Sap1, a protein that binds to sequences required for mating-type switching, is essential for viability in *Schizosaccharomyces pombe*. *Mol Cell Biol* 14:2058–2065. <https://doi.org/10.1128/mcb.14.3.2058-2065.1994>.
189. de Lahondès R, Ribes V, Arcangioli B. 2003. Fission yeast Sap1 protein is essential for chromosome stability. *Eukaryot Cell* 2:910–921. <https://doi.org/10.1128/EC.2.5.910-921.2003>.
190. D'Ambrosio C, Schmidt CK, Katou Y, Kelly G, Itoh T, Shirahige K, Uhlmann F. 2008. Identification of cis-acting sites for condensin loading onto budding yeast chromosomes. *Genes Dev* 22:2215–2227. <https://doi.org/10.1101/gad.1675708>.
191. Haeusler RA, Pratt-Hyatt M, Good PD, Gipson TA, Engelke DR. 2008. Clustering of yeast tRNA genes is mediated by specific association of condensin

- with tRNA gene transcription complexes. *Genes Dev* 22:2204–2214. <https://doi.org/10.1101/gad.1675908>.
192. Ekwall K, Nielsen O, Ruusala T. 1991. Repression of a mating type cassette in the fission yeast by four DNA elements. *Yeast* 7:745–755. <https://doi.org/10.1002/yea.320070709>.
 193. Hayashi MT, Takahashi TS, Nakagawa T, Nakayama J, Masukata H. 2009. The heterochromatin protein Swi6/HP1 activates replication origins at the pericentromeric region and silent mating-type locus. *Nat Cell Biol* 11:357–362. <https://doi.org/10.1038/ncb1845>.
 194. Thon G, Hansen KR, Altes SP, Sidhu D, Singh G, Verhein-Hansen J, Bonaduce MJ, Klar AJS. 2005. The Clr7 and Clr8 directionality factors and the Pcu4 cullin mediate heterochromatin formation in the fission yeast *Schizosaccharomyces pombe*. *Genetics* 171:1583–1595. <https://doi.org/10.1534/genetics.105.048298>.
 195. Yamane K, Mizuguchi T, Cui B, Zofall M, Noma K, Grewal SIS. 2011. Asf1/HIRA facilitate global histone deacetylation and associate with HP1 to promote nucleosome occupancy at heterochromatic loci. *Mol Cell* 41:56–66. <https://doi.org/10.1016/j.molcel.2010.12.009>.
 196. Jahn LJ, Mason B, Brøgger P, Toteva T, Nielsen DK, Thon G. 2018. Dependency of heterochromatin domains on replication factors. *G3 (Bethesda)* 8:477–489. <https://doi.org/10.1534/g3.117.300341>.
 197. Chen ES, Zhang K, Nicolas E, Cam HP, Zofall M, Grewal SIS. 2008. Cell cycle control of centromeric repeat transcription and heterochromatin assembly. *Nature* 451:734–737. <https://doi.org/10.1038/nature06561>.
 198. Kloc A, Zaratiegui M, Nora E, Martienssen R. 2008. RNA interference guides histone modification during the S phase of chromosomal replication. *Curr Biol* 18:490–495. <https://doi.org/10.1016/j.cub.2008.03.016>.
 199. Zaratiegui M, Castel SE, Irvine DV, Kloc A, Ren J, Li F, de Castro E, Marín L, Chang A-Y, Goto D, Cande WZ, Antequera F, Arcangioli B, Martienssen RA. 2011. RNAi promotes heterochromatic silencing through replication-coupled release of RNA Pol II. *Nature* 479:135–138. <https://doi.org/10.1038/nature10501>.
 200. Singh G, Klar AJS. 2002. The 2.1-kb inverted repeat DNA sequences flank the mat2,3 silent region in two species of *Schizosaccharomyces pombe* and are involved in epigenetic silencing in *Schizosaccharomyces pombe*. *Genetics* 162:591–602. <https://doi.org/10.1093/genetics/162.2.591>.
 201. Krassowski T, Kominek J, Shen X-X, Opulente DA, Zhou X, Rokas A, Hittinger CT, Wolfe KH. 2019. Multiple reinventions of mating-type switching during budding yeast evolution. *Curr Biol* 29:2555–2562.e8. <https://doi.org/10.1016/j.cub.2019.06.056>.
 202. Sugiyama T, Cam HP, Sugiyama R, Noma K, Zofall M, Kobayashi R, Grewal SIS. 2007. SHREC, an effector complex for heterochromatic transcriptional silencing. *Cell* 128:491–504. <https://doi.org/10.1016/j.cell.2006.12.035>.
 203. Egel R, Beach DH, Klar AJ. 1984. Genes required for initiation and resolution steps of mating-type switching in fission yeast. *Proc Natl Acad Sci U S A* 81:3481–3485. <https://doi.org/10.1073/pnas.81.11.3481>.
 204. Lorentz A, Ostermann K, Fleck O, Schmidt H. 1994. Switching gene swi6, involved in repression of silent mating-type loci in fission yeast, encodes a homologue of chromatin-associated proteins from *Drosophila* and mammals. *Gene* 143:139–143. [https://doi.org/10.1016/0378-1119\(94\)90619-x](https://doi.org/10.1016/0378-1119(94)90619-x).
 205. Jia S, Yamada T, Grewal SIS. 2004. Heterochromatin regulates cell type-specific long-range chromatin interactions essential for directed recombination. *Cell* 119:469–480. <https://doi.org/10.1016/j.cell.2004.10.020>.
 206. Ivanova AV, Bonaduce MJ, Ivanov SV, Klar AJS. 1998. The chromo and SET domains of the Clr4 protein are essential for silencing in fission yeast. *Nat Genet* 19:192–195. <https://doi.org/10.1038/566>.
 207. Akamatsu Y, Dziadkowiec D, Ikeguchi M, Shinagawa H, Iwasaki H. 2003. Two different Swi5-containing protein complexes are involved in mating-type switching and recombination repair in fission yeast. *Proc Natl Acad Sci U S A* 100:15770–15775. <https://doi.org/10.1073/pnas.2632890100>.
 208. Ellermeier C, Schmidt H, Smith GR. 2004. Swi5 acts in meiotic DNA joint molecule formation in *Schizosaccharomyces pombe*. *Genetics* 168:1891–1898. <https://doi.org/10.1534/genetics.104.034280>.
 209. Kurokawa Y, Murayama Y, Haruta-Takahashi N, Urabe I, Iwasaki H. 2008. Reconstitution of DNA strand exchange mediated by Rhp51 recombinase and two mediators. *PLoS Biol* 6:e88. <https://doi.org/10.1371/journal.pbio.0060088>.
 210. Aguilar-Arnal L, Marsellach F, Azorín F. 2008. The fission yeast homologue of CENP-B, Abp1, regulates directionality of mating-type switching. *EMBO J* 27:1029–1038. <https://doi.org/10.1038/emboj.2008.53>.
 211. Matsuda E, Sugioka-Sugiyama R, Mizuguchi T, Mehta S, Cui B, Grewal SIS. 2011. A homolog of male sex-determining factor SRY cooperates with a transposon-derived CENP-B protein to control sex-specific directed recombination. *Proc Natl Acad Sci U S A* 108:18754–18759. <https://doi.org/10.1073/pnas.1109988108>.
 212. Yu C, Bonaduce MJ, Klar AJS. 2012. Going in the right direction: mating-type switching of *Schizosaccharomyces pombe* is controlled by judicious expression of two different swi2 transcripts. *Genetics* 190:977–987. <https://doi.org/10.1534/genetics.111.137109>.
 213. Noma K, Allis CD, Grewal SIS. 2001. Transitions in distinct histone H3 methylation patterns at the heterochromatin domain boundaries. *Science* 293:1150–1155. <https://doi.org/10.1126/science.1064150>.
 214. Thon G, Maki T, Haber JE, Iwasaki H. 2019. Mating-type switching by homology-directed recombinational repair: a matter of choice. *Curr Genet* 65:351–362. <https://doi.org/10.1007/s00294-018-0900-2>.
 215. Parvanov E, Kohli J, Ludin K. 2008. The mating-type-related bias of gene conversion in *Schizosaccharomyces pombe*. *Genetics* 180:1859–1868. <https://doi.org/10.1534/genetics.108.093005>.
 216. Armakolas A, Klar AJS. 2006. Cell type regulates selective segregation of mouse chromosome 7 DNA strands in mitosis. *Science* 311:1146–1149. <https://doi.org/10.1126/science.1120519>.
 217. Cairns J. 1975. Mutation selection and the natural history of cancer. *Nature* 255:197–200. <https://doi.org/10.1038/255197a0>.
 218. Yu C, Bonaduce MJ, Klar AJS. 2013. Defining the epigenetic mechanism of asymmetric cell division of *Schizosaccharomyces japonicus* yeast. *Genetics* 193:85–94. <https://doi.org/10.1534/genetics.112.146233>.